[AMERICAN JOURNAL OF SCIENCE, VOL. 298, JUNE, 1998, P. 471–498]

# NATURAL FLUID-DEPOSITED GRAPHITE: MINERALOGICAL CHARACTERISTICS AND MECHANISMS OF FORMATION

F. J. LUQUE,* J. D. PASTERIS,** B. WOPENKA,** M. RODAS,* and J. F. BARRENECHEA*

**ABSTRACT. This paper focuses on the similarities and differences between metamorphic graphite (formed *in situ* from organic matter) and fluid-deposited graphite. We discuss the formation of fluid-deposited graphite in terms of the source of carbon, the characteristics of the C-bearing fluids (the C–O–H system), the mechanisms of carbon mobilization, and the mechanisms of carbon precipitation. New and existing analytical data are compiled on the physical and chemical characteristics of fluid-deposited graphite obtained by the following techniques: optical microscopy, differential thermal analysis, thermogravimetry, X ray diffraction, Raman spectroscopy, and stable isotope mass spectrometry. Our discussions focus on major, that is, volumetrically significant, worldwide concentrations of graphite.**

## INTRODUCTION

Graphite commonly occurs in metasedimentary rocks as a result of the conversion of organic matter through regional or contact metamorphism. From diagenesis to the uppermost metamorphic grades, the organic material passes through a series of intermediate forms, terminating in fully ordered graphite. The stage in the evolution of organic matter into graphite, that is, its degree of graphitization, is governed mainly by temperature, duration of metamorphism, and lithology of the host rock, with lesser control by pressure. At the lowest P-T range, shear stress and variations in the starting material also appear to play significant roles in the degree of graphitization (Diessel, Brothers, and Black, 1978; Wintsch and others, 1981; Bonijoly, Oberlin, and Oberlin, 1982; Ross and Bustin, 1990). It also is recognized that some types of organic matter are inherently very difficult to graphitize (Oberlin, Boulmier, and Villey, 1980; Beny-Bassez and Rouzaud, 1985; Large, Christy, and Fallick, 1994).

Graphitization of organic matter is moderately well understood and can be described in terms of mineralogical, physical, and chemical changes. Diverse analytical techniques have been applied to monitoring such physico-chemical changes: optical microscopy (Diessel and Offler, 1975), X-ray diffraction (Landis, 1971; Grew, 1974; Kwiecinska, 1980; Itaya, 1981; Wang, 1989; Oh and others, 1991), differential thermal analysis (Kwiecinska, 1980; Wada and others, 1994), transmission electron microscopy (Buseck and Huang, 1985; Oh and others, 1991), Raman spectroscopy (Tuinstra and Koenig, 1970; Beny-Bassez and Rouzaud, 1985; Pasteris and Wopenka, 1991; Wopenka and Pasteris, 1993), and stable carbon isotopic analysis (Hoefs and Frey, 1976; Weis, Friedman, and Gleason, 1981; Dunn and Valley, 1992).

However, the heating and compression of organic matter *in situ* is only one of the ways in which graphite is produced in nature. The other way is the precipitation of solid carbon (that is, "graphite") from natural carbon-bearing fluids such as those containing $CO_2$, CO, and/or $CH_4$. Although graphite of metamorphic origin has been studied in great detail, there is not a comprehensive review of such fluid-deposited graphite. The present paper summarizes the natural occurrences and the mineralogical, crystalchemical, and isotopic characteristics of graphite precipitated from carbon-saturated fluids in geological environments. The discussion focuses on volumetrically large graphite deposits, although some inferences are drawn from small-scale graphite precipitates. The goals are (1) to present a wide array of analytical data, some presented for the first time, on

* Departamento de Cristalografía y Mineralogía, Facultad de Geologia, Universidad Complutense de Madrid, 28040 Madrid, Spain

** Department of Earth and Planetary Sciences, Washington University, Campus Box 1169, St. Louis, Missouri 63130

fluid-deposited graphite from worldwide localities, (2) to consider, on the basis of analytical parameters, whether graphite that formed by fluid deposition is different from graphite of metamorphic origin, and (3) to investigate if fluid-deposited graphite is characterized by any physical and chemical property that would be a useful indicator of the specific conditions of the graphite's origin.

Geologically, there are several reasons why one would want to learn more about fluid-deposited graphite. An obvious impetus is to derive appropriate temperature-crystallinity correlations so that the depositional temperature can be inferred from graphite deposits. The structural state of graphite is also important because it both affects and is controlled by: the kinetics of graphite precipitation, the degree of supersaturation of a C-O-H fluid before graphite precipitates, and the physical form of the graphite as it ultimately precipitates. The physical properties of graphite films in fractures will affect their physical connectivity and other parameters that control electrical conductivity. Such factors are essential to the understanding of electrical conductivity measurements made on deep crustal materials (Duba and Shankland, 1982; Frost and others, 1989; Mathez and others, 1995; Yardley and Valley, 1997). The fluid-deposition and -resorption of graphite also control the mobility of carbon in the crust and mantle, as well as the "stability" (longevity) of carbon films (Mathez, 1987; Tingle, Mathez, and Hochella, 1991; Sugisaki and Mimura, 1994). Larger-scale deposition of graphite, particularly in granulite terranes, drew attention to the possibility of regional infiltration by large volumes of $CO_2$ and to the oxygen fugacities necessary to stabilize graphite under those metamorphic conditions (Newton, Smith, and Windley, 1980; Glassley, 1982; Lamb and Valley, 1984; Katz, 1987; Dissanayake, 1994). In contrast, the fluid-deposition of huge deposits of graphite has not yet been the focus of major petrologic analysis but rather has been considered more of an economic geology issue. In addition to being ore deposits, however, these graphite accumulations are also the physical and chemical records of the passage of huge volumes of carbon-bearing fluids through the crust for large amounts of time.

## CRYSTALLOGRAPHIC ASPECTS OF GRAPHITE

An important physical aspect of graphite crystals is their size on both the microscopic and macroscopic levels. In an ideal graphite crystal, the 6-fold ring of carbon atoms is repeated perfectly and extends infinitely within the basal plane; these planes in turn are spaced equidistantly in stacks that extend infinitely in a direction perpendicular to the planes themselves. Two types of repetitions of carbon layers are possible within the graphite structure, resulting in either the hexagonal (stacking sequence ABABAB . . .) or the rhombohedral (stacking sequence ABCABC . . .) polytypes. The hexagonal phase is strongly dominant over the rhombohedral phase in all known natural cases. In natural crystals, there are defects and dislocations that limit the length scale of crystalline perfection in different directions. The length scales of ordering (crystal perfection) are measured along the a-axis (measured parameter is $L_a$) and the c-axis ($L_c$). Well-crystallized graphite is crystallographically defined by an interplanar d value of exactly 3.35 Å and is on the order of at least several hundreds to a thousand Ångströms each for $L_a$ and $L_c$. Solid carbon phases with $d_{(002)} > 3.35$ Å and smaller crystallite sizes are referred to as "disordered graphite." The size of the ordered graphite domains is referred to as the *crystallite size.* A different, although usually related, physical parameter is the *grain size,* which refers to the macroscopically measurable size of the graphite flakes or granules.

For graphite formed by the metamorphism of organic matter, both crystallite size and grain size are strongly affected by the conditions of formation or recrystallization of the carbonaceous phase. The relation between the genesis and the crystallographic properties of such graphite is clear: heteroatoms such as oxygen, hydrogen, and nitrogen

are released incrementally during metamorphism (especially due to heating), and the residual carbon atoms are stacked progressively into three-dimensional planar arrays of 6-fold rings. As this process progresses, the distance between the planes ($d_{(002)}$) decreases to the ideal value of about 3.35 Å, and the crystallite size also increases until $L_a$ and $L_c$ are on the order of thousands of Ångströms or more. The graphite exhibits an increasingly higher degree of ordering (see, for example, Diessel and Offler, 1975; Kwiecinska, 1980; Wada and others, 1994). This maturation mechanism allows for the degree of crystallinity of metamorphic graphite to be a reasonably reliable indicator of its conditions of formation, especially of the thermal history of the enclosing rock, provided that the organic precursor is graphitizable (see for example, discussions in Grew, 1974; Buseck and Huang, 1985; Wopenka and Pasteris, 1993; Large, Christy, and Fallick, 1994). It must be noted that once graphite has attained a certain degree of ordering/crystallinity, it does not retrograde during subsequent metamorphism. Graphite is one of the few single-mineral geothermometers (see for example, discussions in Luque, Barrenechea, and Rodas, 1993).

## GEOLOGIC OCCURRENCES OF FLUID-DEPOSITED GRAPHITE

Occurrences of fluid-deposited graphite can be categorized on the basis of parameters such as the volume of the deposit (from minable concentrations down to thin films), host-rock lithology, structural relation between the graphite and its host (concordant, discordant), graphite:host volumetric ratio (for example, massive or disseminated graphite), morphology of the graphite (for example, isolated blades, spherulites, massive fine-grained), degree of crystallinity of the graphite (crystallite size), and composition (wt percent C, $\delta^{13}C$, higher hydrocarbon content).

The main types of fluid-deposited graphite can be grouped into: (A) veins, (B) replacement deposits, and (C) disseminations in plutonic rocks (mainly mafic to ultramafic). The term "disseminations" is used here to designate graphite that is dispersed (not channel controlled, as in veins), that is, physically isolated crystals or aggregates randomly distributed throughout the rock. Our use of the term disseminations encompasses a wide range of total carbon contents (up to those typically termed massive). Less abundant types of fluid-deposited graphite are (D) stringers and patches in mantle xenoliths, (E) coatings and films in vesicles and microcracks of submarine basaltic rocks, and (F) deposits in fluid inclusions.

Some well known geologic occurrences of fluid-deposited graphite are summarized in table 1. Vein-type graphite (type A) is the most important occurrence. Until recently, this type was thought to be restricted to high-grade metamorphic rocks of Precambrian age (Goossens, 1982), but vein-type graphite deposits actually have a wide range in age (see table 1). The vein deposits display a number of common features in that they range in thickness from a few millimeters to several meters and cross cut the rock fabric in simple veins or stockworks. In their macroscopic morphology, the graphite crystals usually occur as parallel or radiating aggregates that are perpendicular to the vein walls. Typically, graphite is also present as disseminated flakes in the metasedimentary host rocks (Erdosh, 1970, 1972; Acharya and Dash, 1984; Katz, 1987; Dissanayake, 1994). The well known vein-graphite mineralizations of Sri Lanka and India are estimated to have formed at temperatures of about 750°C (Katz, 1987) and 650° to 850°C (Acharya and Dash, 1984), respectively.

Younger vein-type mineralizations of historic economic interest occur in mafic-ultramafic rocks, including those associated with the Miocene lherzolitic rocks of the Serranía de Ronda (Betic Cordillera, southern Spain) and Beni-Bousera (Morocco) and with Jurassic alkaline basalts near Huelma in the external parts of the Betic Cordillera (southern Spain) (Gervilla, 1989; Luque, Rodas, and Galán, 1992; Barrenechea and others, 1997). Other vein-graphite occurrences also have been described in acid-

TABLE 1

*Occurrences of fluid-deposited graphite*

| # | Locality | Host Rock | Age | Type of Occurr. | Mineral Association* | Graph. Morphol. | Graph. Cont. (%) | Carbon Cont. (%) | Est. Form. T (°C) | DTA Max. (°C) | $d_{(002)}$ (Å) | Raman D/O ratio | Rhom. Graph. (%) | $\delta^{13}C$ (‰) | Inferred Origin for Carbon | Reference |
|---|---|---|---|---|---|---|---|---|---|---|---|---|---|---|---|---|
| 1 | Sri Lanka | Granulite- and amph-facies metaseds. | Precambrian | vein and stock-work | *± Q ± Py* | flakes and spherul. | up to 100 | >99 | 750 | 860 | 3.35-3.36 | 0.04 | 3-21 | -7.1 to -9.0 | $CO_2$ infiltration of deep crustal carbon | Dobner and others, 1978; Katz, 1987; Dissanayake, 1981; 1994; Wopenka and Pasteris, 1993. |
| 2 | Kerala and Orissa (India) | granulite-facies metaseds. and calcsilicates | Precambrian | vein | *Q ± KF ± Plg ± Gt ± Sill ± Cd* | flakes, masses | up to 100 | -- | 650-850 | 900 | 3.37 | -- | -- | -8.6 to -13.4 | $CO_2$ infiltration of deep crustal carbon | Acharya and Dash, 1984; Soman, Lobzova and Sivadas, 1986; Santosh and Wada, 1993. |
| 3 | Dillon, Montana (USA) | gneisses | Precambrian | vein and stock-work | *Ab ± Q* | flakes, needles, rosettes | up to 100 | -- | 600 | -- | -- | <0.1 | -- | -5.8 to -8.6 | $CO_2$-$CH_4$ infiltration; devolatilization of marble | Ford, 1954; Cameron and Weis, 1960; Weis and others, 1981; Duke, Galbreath, and Trusty, 1990; this work. |
| 4 | Duluth Complex, Minnesota (USA) | serpentinized ultramafics within troctolites | Precambrian | vein ? and dissem. | *± Cu-Fe sulfides* | flakes | -- | -- | -- | -- | -- | -- | -- | -- | assimilation of organic seds. | Hollister, 1980. |
| 5 | New Hampshire (USA) | granite-quartz diorite; sill-grade metaseds. | Silurian-Devonian | vein ? | *Q + Tm + Ms + Chl + Sill + Fe-Ti ox* | flakes and spherul. | up to 100 | -- | 600 | -- | -- | -- | -- | -9 to -28 | fluid mixing during metam. + hydrotherm. processes | Duke and Rumble, 1986; Rumble and Hoering, 1986; Rumble, Duke, and Hoering, 1986. |
| 6 | Huelma, Betic Cordillera (Spain) | alkali basalts | Jurassic | vein and dissem. | *Ol + Plg + Fe-Ti ox ± Cpx* | flakes | up to 100 | >90 | 700-750 | 780-820 | 3.351-3.356 | 0-0.07 | 0-25 | -20.7 to -23.0 | assimilation of organic seds. | Barrenechea and others, 1997. |
| 7 | British Columbia (Canada) | tholeiitic basalts and black shales | Cretaceous | vein | *Q + Ank + Py* | angular fragments | 95 | 50-90 | 300 | -- | Amorphous | -- | -- | -26.0 to -27.0 | mobilized organic carbon from seds. | Mastalerz, Bustin, and Sinclair, 1995. |
| 8 | Serranía de Ronda (Spain) | lherzolites | Miocene | vein and stock-work | *Chrom + Fe-Ni-Cu sulfides* | flakes and nodules | up to 90 | >95 | 770-820 | 800 | 3.348 | 0-0.08 | 0 | -16.5 to -17.3 | assim. of organic seds. + mixing with igneous melt | Gervilla and Leblanc, 1990; Luque, Rodas, and Galán, 1992; this work. |
| 9 | Beni-Bousera (Morocco) | lherzolites | Miocene | vein and stock-work | *Chrom + Fe-Ni-Cu sulfides* | flakes | up to 100 | up to 100 | 700-725 | -- | 3.352 | -- | 0 | -18.0 | assimilation and mixing | Huvelin and Permingeat, 1980; Gervilla and Leblanc, 1990. |
| 10 | Borrowdale (England) | andesites | Ordovician | re-placement | *Cpx + Opx + Plg ± KF ± Clz ± Fe-su + ox* | flakes, nodules, stringers | 40-85 | 99 | 400-600 | 790 | 3.361 | 0.07-0.25 | 31.9 | -27.2 | assimilation of organic seds. | Strens, 1965; Kwiecinska, 1980; Weis, Friedman, and Gleason, 1981; this work. |

TABLE 1

*(continued)*

| # | Locality | Host Rock | Age | Type of Occurr. | Mineral Association | Graph. Morphol. | Graph. Cont. (%) | Carbon Cont. (%) | Est. Form. T (°C) | DTA Max. (°C) | $d_{(002)}$ (Å) | Raman D/O ratio | Rhom. Graph. (%) | $\delta^{13}C$ (‰) | Inferred Origin for Carbon | Reference |
|---|---|---|---|---|---|---|---|---|---|---|---|---|---|---|---|---|
| 11 | Fish Lake Intrusion, Duluth Complex, MN (USA) | troctolites and gabbros | Precam-brian | re-placement + dissem | *Plg + Chl + Amph + Q* | spherul. | trace | -- | 700+ | -- | -- | 0 | -- | -- | assimilation of organic seds. | Pasteris, Harris, and Sassani, 1995. |
| 12 | Water Hen Intrusion, Duluth Complex, MN (USA) | troctolites, gabbros, and dunites | Precam-brian | re-placement + vein | *Amph ± Cu-Fe sulfides* | blades and fine-gr. massive | up to >90 | -- | >600 | 820 | 3.351 | 0 | 0 | -30.6 | assimilation of organic seds. | Mainwaring and Naldrett, 1977; this work. |
| 13 | Bushveld Complex (South Africa) | pyroxenitic pegmatites | Precam-brian | re-placement + dissem | *Amph + Bi + Chl + sulfides* | flakes and globules | up to > 80 | -- | 500-600 | -- | 3.35 | -- | -- | -21 to -19 | assimilation (and mixing?) | Ballhaus and Stumpfl, 1985; Taylor, 1986. |
| 14 | KTB Hole (Germany) | metagabbros and amphibolites | Carbon-iferous | dissem | *Chl + Plg + KF + Q ± Ms* | flakes and blades | -- | -- | [illegible] | [illegible] | -- | 0.03-0.28 | -- | -20 to -27 | assimilation of organic seds. and mixing | Bartels and Pasteris, 1993; Bartels and others, in prep; this work |
| 15 | Eggéré (Algeria) | ultramafic xenoliths in alkali basalts | Precam. in Plio. Quater. lavas | dissem | *Ol + Opx* | flakes | trace to 0.7 | -- | 400-800 | -- | -- | -- | -- | -14.4 to -24.6 | igneous (mantle-derived) | Pineau, Javoy, and Kornprobst, 1987. |
| 16 | Kimberley (South Africa) | kimberlites | Creta-ceous | dissem | *Ol + Phl* | flakes and spherul. | 6-9 | -- | -- | -- | -- | -- | -- | -- | igneous (mantle-derived) | Pasteris, 1981, 1988. |
| 17 | Serranía de Ronda (Spain) | acid dikes in lherzolites | Miocene | dissem | *Cd + Q + Bi + Gt + Plg + Fe-Ti ox* | flakes | 10-15 | >85 | 765-825 | 650-730 | 3.348-3.351 | -- | 0 | -21.3 | Inherited organic carbon | Luque and others, 1987; Luque, Barrenechea, and Rodas, 1993. |
| 18 | Serranía de Ronda (Spain) and Beni-Bousera (Morocco) | garnet clino-pyroxenite | Miocene | dissem | *Gt + Cpx ± Plg ± Sp ± sulfides* | octah.+ cubic forms | up to 25 | -- | >900 | 820 | 3.351 | 0 | 0 | -- | igneous (mantle-derived) | Pearson and others, 1989; Davies and others, 1993; this work. |

Localities are grouped by occurrence type (column 5). These particular mineralizations were chosen due to the abundance of physical data available on them and their representation of occurrence type. Locality names reflect general geographic area. More than one type of graphite deposite may occur in that area, leading to multiple entries in the table. Metamorphic graphite occurs in some of the same localities as the [illegible] graphite described here.

*) The mineral associations indicate the phases [illegible] graphite in the veins (in italics) or the primary mineral assemblage of the host rock when graphite is disseminated or occurs as replacements. Abbreviations: Ab = Albite, Amph = Amphibole, Ank = Ankerite, Bi = Biotite, Cd = Cordierite, Chl = Chlorite, Chrom = Chromite, Ciz = Clinozoisite, Cpx = Clinopyroxene, KF = K-feldspar, Gt = Gamet, Ms = Muscovite, Ol = Olivine, Opx = Orthopyroxene, Ox = oxides, Phl = Phlogopite, Pig = Plagioclase feldspar, Py = Pyrite, Q = Quartz, Sill = Sillimanite, Sp = Spinel, Su = Sulfides, Tm = Tourmaline.

--.....no data available.

intermediate igneous rocks associated with Paleozoic granite-quartz diorite rocks from south-central New Hampshire (Duke and Rumble, 1986). Graphite occurs in recognized hydrothermal veins of various ages, including those that cross cut both plutons and their surrounding metasediments in New Hampshire (Rumble, Duke, and Hoering, 1986; Rumble and Hoering, 1986), and with hydrothermal gold-quartz vein deposits in an allochthonous terrane in northern British Columbia, Canada (Mastalerz, Bustin, and Sinclair, 1995). Finally, graphite crystals have been reported in some modern hydrothermal systems, for instance, in association with sulfoantimonides in hydrothermal vents on the seafloor (Jedwab and Boulegue, 1984).

Deposition of graphite from fluids also results from fluid-rock interactions that lead to massive replacement (type B), typically of silicate material, or to disseminations (type C) that may co-precipitate with other minerals. The purported massive replacement mineralization at Borrowdale, England (Strens, 1965; Weis, Friedman, and Gleason, 1981) occurs as irregular to nodular graphite concentrations (up to 0.6 m, but typically 2–20 mm diam) within hydrothermally altered andesitic rocks of Ordovician age. Textural evidence shows that graphite replaces orthoclase, albite, and clinozoisite of the host rock and probably formed at temperatures of 400° to 600°C (Strens, 1965). The fluid-deposited graphite occurrences described as "disseminated" (type C) are different from macroscopic vein-like or other massive deposits. However, some of them share important features with the "replacement deposits" except for their variable to low concentration of graphite. These mineralizations range in age and are characterized by isolated flakes, fine stringers, spherulites, and intergrowths with hydrous silicate minerals. Disseminated graphite is associated with igneous rocks ranging in composition from granitic to ultramafic, although its localization and physical form commonly appear lithologically controlled.

Occurrences of type C can be gradational into more massive graphite concentrations (Ballhaus and Stumpfl, 1985; Reutel, Skrotzki, and Vollbrecht, 1989) and can reflect their carbon source. For instance, octahedral crystals of graphite, which occur disseminated in some pyroxenitic rocks of the Beni Bousera ultramafic complex in Morocco, are pseudomorphic after diamond and reflect the mantle history of these rocks (Pearson and others, 1989; Davies and others, 1993). Fluid-deposited graphite also occurs as disseminations in anatectic acid dikes cutting across the lherzolitic rocks (themselves containing graphite veins) of the tectonically related Serranía de Ronda ultramafic complex of Spain (Luque and others, 1987; Luque, Barrenechea, and Rodas, 1993).

Massive to dispersed occurrences of graphite have been reported in pyroxene pegmatites in the Bushveld Complex (interpreted as post-cumulus alteration products; Ballhaus and Stumpfl, 1985) and Stillwater Complex (interpreted as primary precipitates from a fluid phase; Volborth and Housley, 1984; Mathez and others, 1989). The most massive "disseminated" graphite deposits in the Bushveld Complex, of the "pothole" type, are gradational into replacement deposits (type B).

Graphite disseminations have developed during hydrous alteration of igneous rocks. For instance, in troctolites of the Duluth Complex of Minnesota, graphite spherulites up to a few millimeters in diameter are intergrown with fine-grained mats of amphibole and chlorite, which have replaced mafic silicate phases (Hollister, 1980; Pasteris, 1989; Pasteris, Harris, and Sassani, 1995). In the mafic to ultramafic Water Hen intrusion within the western edge of the Duluth Complex, coarse-bladed graphite, amphiboles, and Cu-Fe-sulfide phases are intergrown in hydrously altered rocks. These textures suggest a combination of primary fluid deposition and replacement processes for this graphite (Mainwaring and Naldrett, 1977; Pasteris, unpublished data). Finely dispersed graphite and graphite aggregates also have been found in serpentinized kimberlites (Pasteris, 1981) and in hydrously altered igneous and metamorphic rocks from the German continental deep drill (KTB) hole in southeastern Germany (Bartels

and Pasteris, 1993). More massive occurrences of fluid-deposited graphite are found along deep crustal fractures in the KTB hole at several kilometers depth (Reutel, Skrotzki, and Vollbrecht, 1989), which is another example of the gradation of disseminated graphite into more massive graphite.

More rarely documented occurrences of fluid-deposited graphite include stringers and patches (up to several millimeters) in mantle xenoliths (type D) (Pineau, Javoy, and Kornprobst, 1987; Pearson, Boyd, Nixon, 1990; Tingle, Mathez, and Hochella, 1991; Pearson and others, 1994; Schulze and others, 1997), vesicle coatings and microcrack films in submarine basalts and mantle xenoliths (type E) (Mathez and Delaney, 1981; Des Marais and Moore, 1984; Mattey and others, 1984; Mathez, 1987), grain-boundary coatings in crustal rocks (Frost and others, 1989; Jödicke, 1992; Mathez and others, 1995; Stevens, 1997), and graphite precipitates in fluid inclusions (type F) (Pasteris and Wanamaker, 1988; Guilhaumou and others, 1990; Cesare, 1995; Klemd, Bröcker, and Schramm, 1995; Morgan and others, 1993; Pasteris and Chou, 1998).

## PHYSICAL AND CHEMICAL CHARACTERISTICS OF FLUID-DEPOSITED GRAPHITE

### *Determination of optical properties: Reflected-light microscopy*

Reflected-light optical microscopy gives information about the textural and microstructural characteristics of graphite crystals and aggregates. The majority of fluid-deposited graphite consists of medium- to coarse-grained flakes or needles and thus resembles high-grade metamorphic graphite. In most vein-type deposits, the graphite crystals are oriented perpendicular to the vein walls and may show features of sequential deposition (Katz, 1987; Duke, Galbreath, and Trusty, 1990). Coarse graphite crystals also occur in replacement deposits and in some of the disseminated-type deposits. Strained crystals, resulting in wavy extinction, are common due to the high ductility of graphite (fig. 1A). Another noteworthy textural type of fluid-deposited graphite consists of fine-grained rosettes or spherulitic aggregates (fig. 1B) displaying radial arrays. These have been reported both in vein-type mineralizations and in disseminated occurrences (see table 1). Nodules composed of coarse crystals surrounded by thin flakes (fig. 1C) have been reported in the vein deposits of the Serranía de Ronda (Luque, Rodas, and Galán, 1992). More than one of these morphologies may occur within a single occurrence (for example, within a single vein; fig. 1D).

Graphite precipitated from fluids is commonly highly anisotropic and has high $R_{max}$ (maximum reflectance) values, indicative of a high degree of crystallinity. $R_{max}$ values close to 15 percent have been reported for the Sri Lanka and Ticonderoga vein deposits (Diessel and Offler, 1975; Kwiecinska, 1980) and for the vein mineralization associated with volcanic rocks of southern Spain (Luque, Barrenechea, and Rodas, 1994). Indeed, the reflectance values of most fluid-deposited graphite are numerically similar to those obtained from graphite in high-grade metamorphic rocks. An interesting contrast to this generalization is reported by Mastalerz, Bustin, and Sinclair (1995), who studied hydrothermal gold-quartz veins in which the concentrated carbonaceous material is isotropic or weakly anisotropic, indicative of a low state of crystallinity.

### *Determination of Thermal Properties: Differential Thermal Analysis (DTA) and Thermogravimetry (TG)*

The temperature position of the DTA maximum for graphite correlates with the temperature at which the graphite formed (Diessel and Offler, 1975; Kwiecinska, 1980; Wada and others, 1994). Figure 2 shows the DTA-TG curves of fluid-deposited graphite from the Water Hen body on the western edge of the Duluth Complex, Minnesota. As for most fluid-precipitated graphite listed in table 1, the Duluth curve has its maximum in the range 800° to 860°C. According to Kwiecinska (1980), such temperatures are in the same range as the ones determined from DTA maxima for the most crystalline of

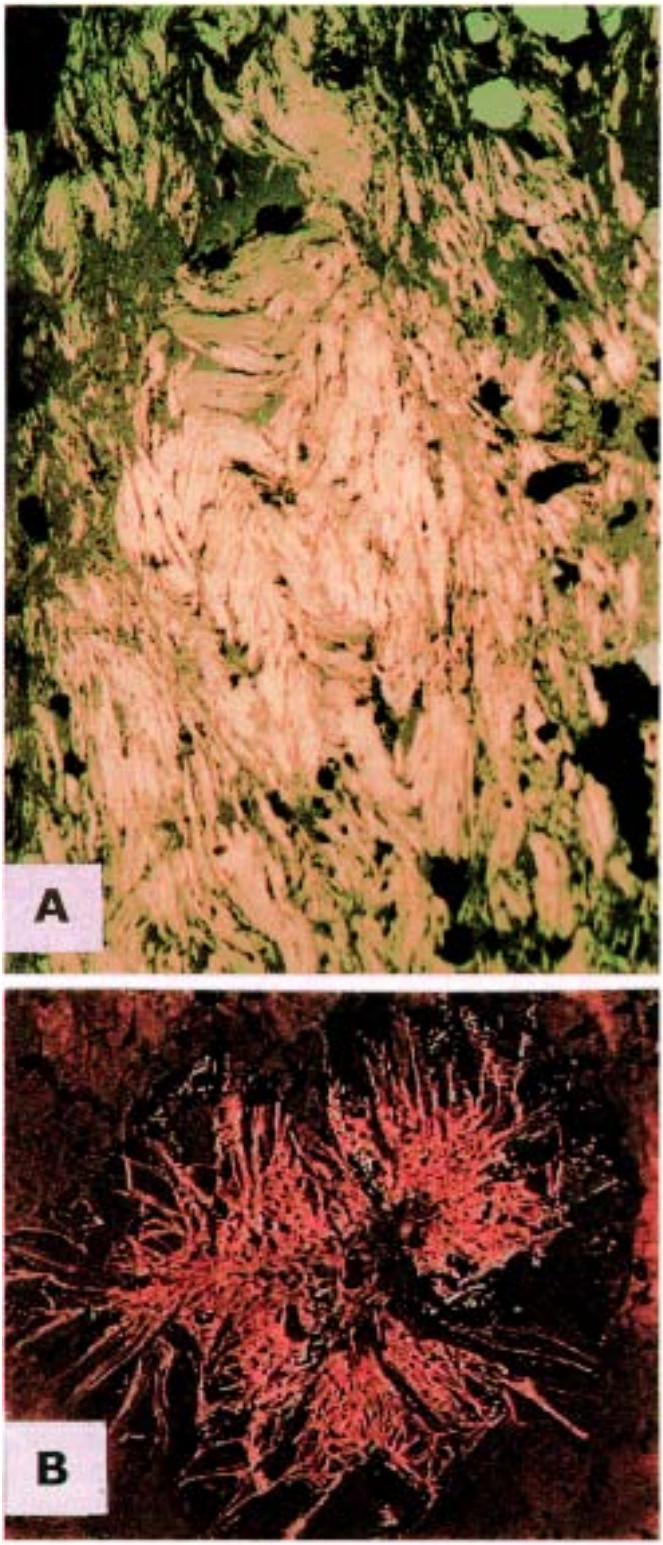


Fig. 1. Examples of the morphology of fluid-deposited graphite in reflected light. (A) Folded laminar crystals from entry #8 in table 1; largest dimension of photo is 1.25 mm. (B) Radial array of needle-like graphite crystals from entry #11 in table 1; largest dimension of photo is 425 µm.

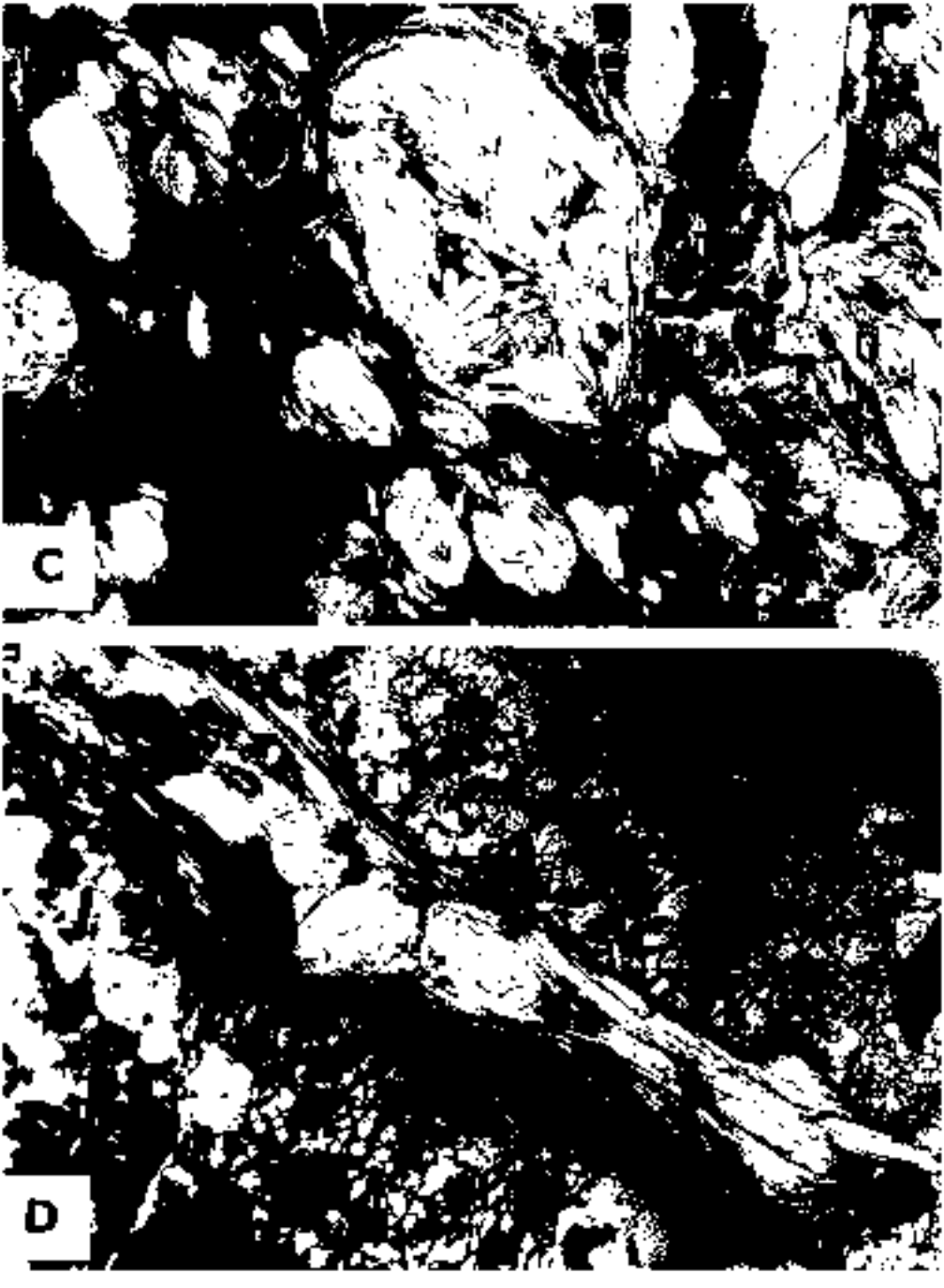


Fig. 1(C) Nodular aggregates formed by thick laminar crystals surrounded by thin flakes from entry #8; largest dimension of photo is 350 μm. (D) Laminated graphite crystals parallel to the vein walls and nodule-like aggregates from entry #8; largest dimension of photo is 2.5 mm.

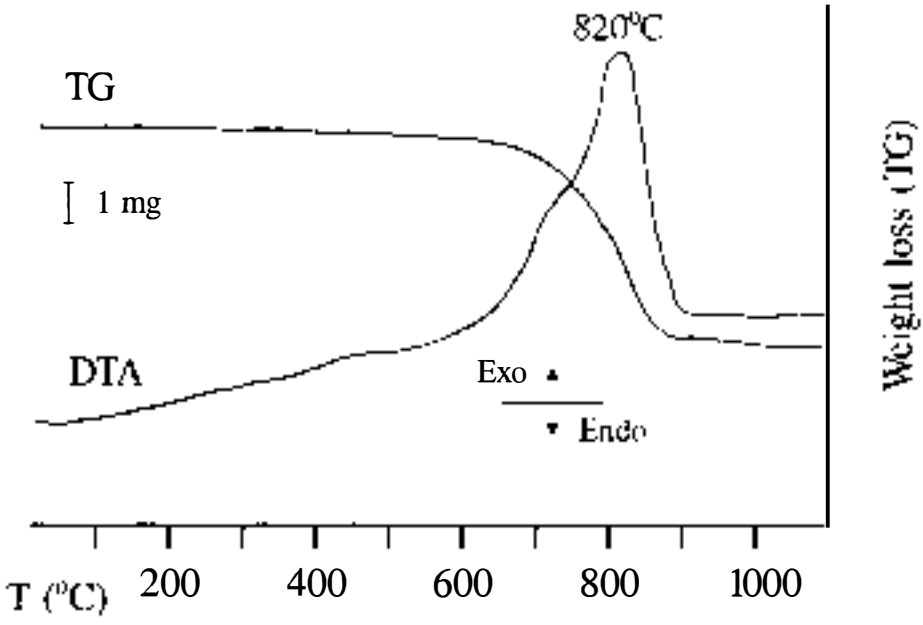


Fig. 2. Differential thermal analysis and thermogravimetric curves for graphite from the Water Hen body (Dr. ll. Complex, entry #12 in table 1), showing the exothermic effect and weight loss due to the combustion of carbon. Initial weight: 9.26 mg.

metamorphic graphite, that is, along the boundary between the amphibolite and granulite facies. Carbon contents calculated from weight loss on the TG curves generally exceed 90 percent for fluid-deposited graphite (table 1) and agree well with C contents determined by elemental analyses (Luque, ms).

### *Structural Characterization: X-ray Diffraction (XRD), Raman Spectroscopy, and High-Resolution Transmission Electron Microscopy (HRTEM)*

*X-ray diffraction.*–X-ray diffraction patterns of graphite precipitated from fluids typically display the characteristics of very well crystalline graphite (see example in fig. 3). The d-spacings for the three main types of fluid-deposited graphite (veins, replacements, and disseminations) are all within the expected range for "fully ordered" graphite (as defined by Landis, 1971), regardless of the type of the deposit (table 1). Indeed, one of the noteworthy contrasts between fluid-deposited and metamorphic graphite is the limited number of fluid-deposited occurrences in which XRD patterns display the characteristics of poorly crystalline graphitic material. Again, one of the exceptions is reported by Mastalerz, Bustin, and Sinclair (1995) who documented XRD patterns corresponding to amorphous to very poorly graphitized carbon in hydrothermal quartz veins.

XRD analysis distinguishes between the two polytypes of graphite (hexagonal and rhombohedral), based on diagnostic reflections in their diffraction patterns. The existence of the rhombohedral phase is inferred from XRD patterns by peaks at 2.08 and 1.97 Å, corresponding to the (101) and (012) reflections of rhombohedral graphite (fig. 3B). The relative amount of the rhombohedral phase can be evaluated through the intensity ratio between those peaks and the (002) and (004) reflections (Kwiecinska, 1980). In metamorphic graphite, the content of the rhombohedral phase decreases as temperature (that is, metamorphic grade) increases (Kwiecinska, 1980). An important

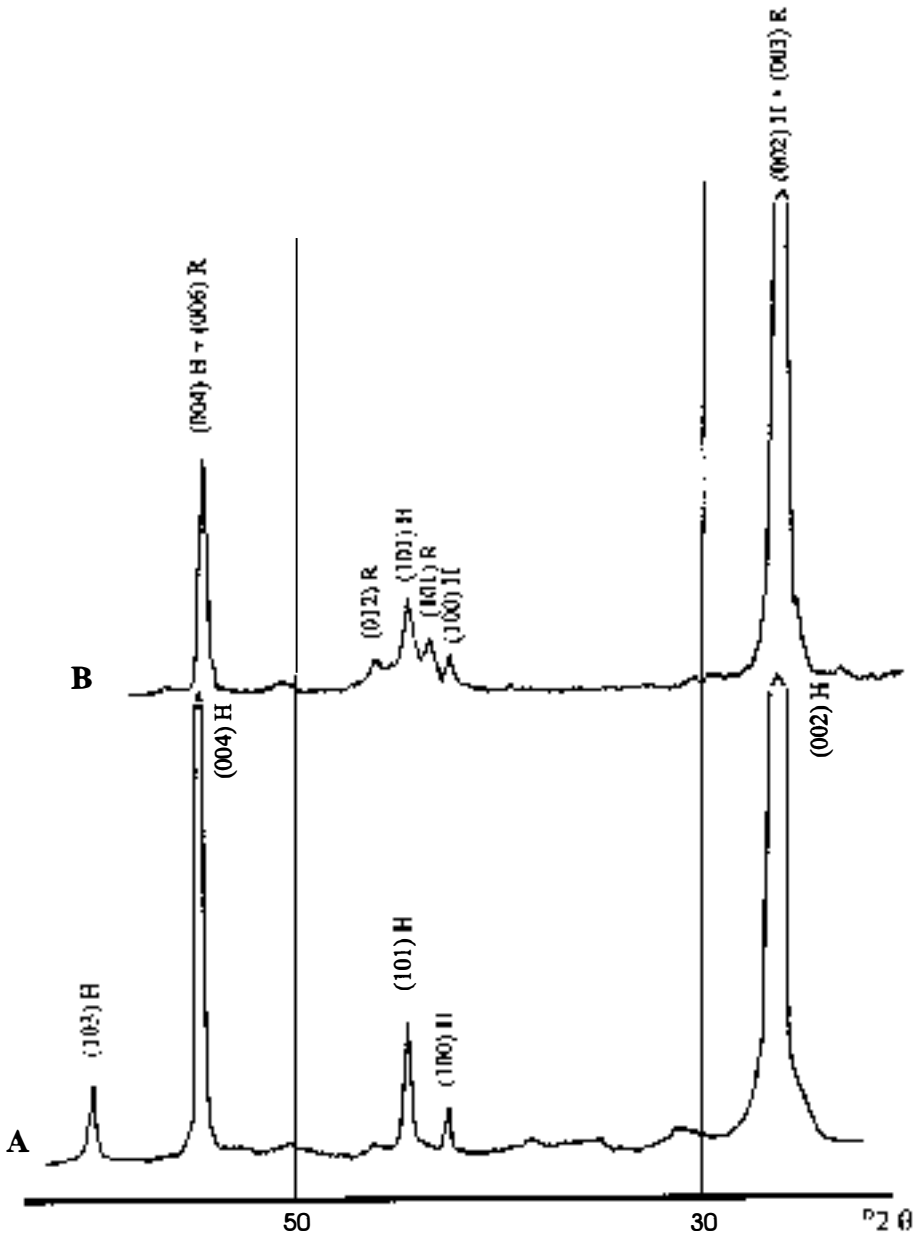


Fig. 3. XRD patterns showing reflections for perfectly ordered hexagonal graphite (H) and rhombohedral graphite (R). (A) vein-graphite from the mineralization of the Betic Cordillera (entry #6 in table 1), which is purely hexagonal, (B) vein-graphite from the same mineralization (entry #6 in table 1) with 25 percent rhombohedral component.

feature revealed in XRD analyses of graphite from many fluid-deposited mineralizations is the presence of a relatively high proportion of the rhombohedral phase (which makes them different from high-grade metamorphic graphite), ranging from 20 to 30 percent in the mineralizations of Sri Lanka, Borrowdale, and Huelma in the Betic Cordillera

(Kwiecinska, 1980; Barrenechea and others, 1997). This finding appears incompatible with the high temperatures of formation estimated for these and most fluid-deposited graphite mineralizations.

*Raman spectroscopy.*–The Raman spectrum of carbonaceous material is sensitive to changes in the degree of ordering as manifested in the in-plane crystallite size $L_a$. The first-order Raman spectrum of well crystalline graphite exhibits a very strong in-plane stretching mode at 1582 $\Delta cm^{-1}$ ("ordered" or "O-peak"). For carbonaceous materials with limited long-range order ("disordered graphite"), the first-order Raman spectrum (fig. 4) shows an additional band at ~1360 $\Delta cm^{-1}$ ("disordered" or "D-peak"). Tuinstra and Koenig (1970) and Beny-Bassez and Rouzaud (1985) showed that the intensity ratio of the D to O peaks is inversely correlated with $L_a$ over a range of ~40 to ~2250 Å (corresponding to our D/O ratios between 1.02 and 0.02), which includes the degree of ordering in natural metamorphosed carbonaceous materials ranging from kerogens and coal to granulite-facies metamorphic graphite. Wopenka and Pasteris (1993) showed that the degree of crystallinity derived from the D/O intensity ratios can be interpreted in terms of metamorphic grade, at least for samples with identical host-rock lithologies.

Figure 4 shows the first- and second-order Raman spectra of six fluid-deposited graphite samples demonstrating a wide range in crystallinity. The top three samples show crystallinities comparable to those of organic matter metamorphosed to granulite-facies conditions, exhibiting crystallite sizes ($L_a$) in excess of 2000 Å. In contrast, the laboratory-produced precipitate shows a crystallinity comparable to that in carbonaceous metapelites from the chlorite zone, exhibiting crystallite sizes on the order of only 20 Å (see Wopenka and Pasteris, 1993).

*Transmission electron microscopy.*–HRTEM studies on carbonaceous materials have focused on graphite of metamorphic origin indicating progressive increase in crystallinity with metamorphic grade (Bonijoly, Oberlin, and Oberlin, 1982; Buseck and Huang, 1985; Beny-Bassez and Rouzaud, 1985; Oh and others, 1991). HRTEM images commonly show that there is structural inhomogeneity both within and among grains from a single graphite sample, even up to medium grades of metamorphism.

There are few structural characterizations of fluid-deposited graphite by means of HRTEM. Available data on the mineralizations from the Serranía de Ronda, both vein-type and disseminated (Luque, 1990; Luque, Rodas, and Galán, 1992), as well as unpublished work by the latter authors on the volcanic-hosted graphite veins from Huelma (Betic Cordillera), suggest that these occurrences are homogeneous at the grain-to-grain scale of the analytical technique. Lattice-fringe images show that these graphite occurrences have a perfectly ordered arrangement of the carbon layers, and that the measured stack heights ($L_c$) agree with the dimensions estimated from XRD reflections. Discrete spots recorded in the electron diffraction patterns (Luque, 1990) also indicate well ordered graphite. The characteristics of both lattice-fringe images and electron diffraction patterns of the fluid-deposited graphite from Serranía de Ronda and Huelma correlate well with those of high-grade metamorphic graphite that demonstrates a high degree of ordering (Buseck and Huang, 1985).

Fluid-deposited graphite associated with cataclastic zones in the KTB hole has been investigated by HRTEM by Reutel and others (1989) and Skrotzki and Reutel (1990). Based on those studies, the crystalline perfection of this graphite can be interpreted as "disordered" and characterized by a high density of lattice defects. Due to the cataclastic environment, it is not clear whether this graphite was fluid-deposited as a poorly ordered phase or whether it was deposited as well ordered graphite that later was disrupted mechanically.

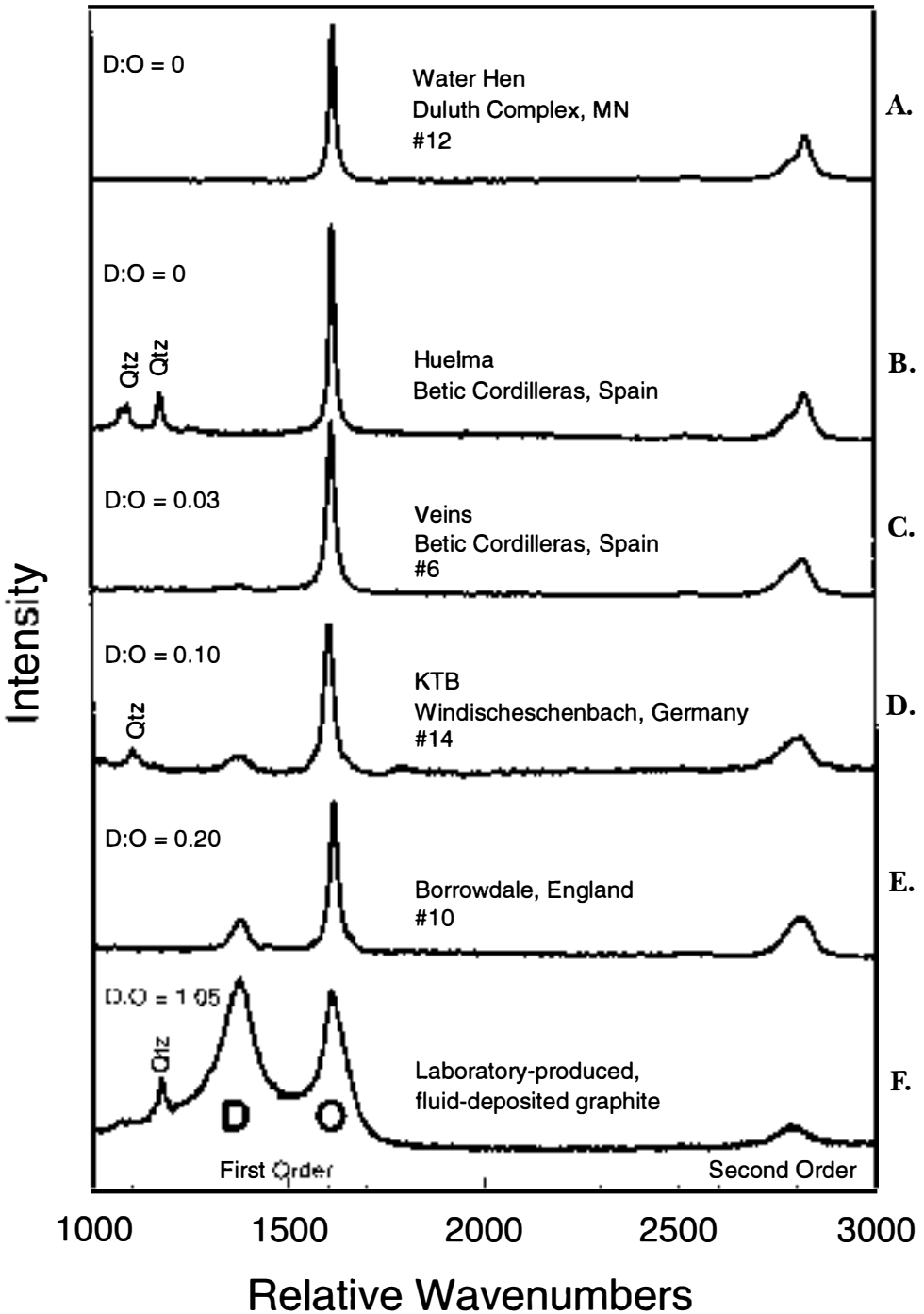


Fig. 4. Raman spectra of fluid-deposited graphite occurrences. Four occurrences are referenced by their entry numbers in table 1. Samples shown in spectra D) and F) are graphite-coated fluid inclusions in quartz. (For more information on the laboratory-produced graphite, see Pasteris and Chou, 1998.) Sample shown in spectrum B) is graphite in a melt inclusion in quartz. (For more information on the Huelma sample, see Barrenechea and others 1997.) All other samples analyzed as grains from vein material.

### *Geochemical Characterization: Determination of the Elemental Composition (C, O, H, N) and Isotopic Signature ($^{13}C/^{12}C$ ratio)*

*Elemental and isotopic composition.*–Table 1 lists carbon contents of fluid-deposited graphite that vary widely but range up to >99 wt percent. The isotopic variations in graphite from metamorphosed rocks have been studied by numerous workers. Comprehensive reviews can be found in Hoefs and Frey (1976), Hahn-Weinheimer and Hirner (1981), Weis, Friedman, and Gleason (1981), Dissanayake (1981), Arneth and others (1985), and Wada and others (1994), among others. Due to the confounding effects of isotopic fractionation and isotopic exchange during graphite formation, carbon isotopic analysis is better suited to identifying the geochemical heritage of the carbon (that is, the carbon source) than to elucidating the mechanism of graphite deposition (that is, distinction between metamorphic and fluid-deposited graphite). For instance, based on their isotopic analyses, Weis, Friedman, and Gleason (1981) emphasized that a large proportion of fluid-deposited carbon was derived from organic compounds in metasediments. The $\delta^{13}$ C values for graphite precipitated from fluids span a wide range (table 1). Isotopic zoning and small isotopic shifts at the millimeter-scale are common features of many fluid-deposited graphite occurrences (Duke and Rumble, 1986; Rumble and Hoering, 1986; Rumble, Duke, and Hoering, 1986).

## MECHANISMS OF FORMATION OF FLUID-DEPOSITED GRAPHITE

The mechanisms discussed below are those expected in the equilibrium precipitation of graphite. We do not have an independent means of evaluating the kinetic pathways that led to the formation of the natural fluid-deposited graphite described in this paper. Some insight into the depositional kinetics is provided by laboratory studies (see later section). We believe that the long times of elevated temperatures experienced by most of the graphite occurrences discussed here have produced equilibrium degrees of crystallinity in most cases. Nevertheless, metastable persistence of a structural type (rhombohedral over hexagonal) apparently occurs in some of the cases discussed.

*The source of carbon.*–Three potential sources of carbon in C–O–H fluids can be envisaged: (1) that from C-bearing compounds released during maturation of organic matter, (2) that from C-bearing compounds released during devolatilization of carbonate-rich materials, and (3) igneous (mainly mantle-derived) carbon. Any attempt to establish the source of carbon for fluid-precipitated graphite should address the influence of the host-rock lithologies. Since fluid-deposited graphite is found in a wide variety of geological settings (see table 1), it is difficult to elucidate the origin of carbon and the mechanisms of mobilization and precipitation based solely on field criteria. Rather, one must consider all the available mineralogical and geological evidence together with geochemical data of fluid-deposited graphite in order to infer the probable source of carbon. Carbon isotopic analysis can help reveal the contributions of the three possible carbon sources (organic matter, carbonates, and igneous carbon of mantle origin) based on the known ranges in isotopic composition for these three reservoirs and the known isotopic effects caused by fractionation between coexisting carbon-bearing species.

The mobility of a carbon-bearing fluid permits it to have "seen" many reservoirs and to have equilibrated with carbon-bearing phases that do not occur near the immediate site of deposition. Fluctuations in the carbon isotope ratio can occur within a single fluid-precipitated graphite deposit, reflecting different episodes of graphite formation, that is, different compositions of the fluids, or different P, T, and $fO_2$ during precipitation. It is even possible that later, fluid-deposited graphite may occur as overgrowths on metamorphic graphite (S. Dunn, personal communication, 1998). Such processes result in millimeter-scale isotopic zoning or in differences in the $^{13}C/^{12}C$ ratio among successive, texturally distinct graphite generations (Duke and Rumble, 1986; Rumble and Hoering, 1986; Rumble, Duke, and Hoering, 1986).

There are several, often geologically inter-related, controls on the isotopic composition of graphite precipitated from fluids. The isotopic signature depends not only on the source(s) of the fluid(s) but also on the fractionation between the existing carbon-bearing species, the latter of which is controlled by the oxidation state of the fluid (speciated into, for example, $CH_4$, $CO_2$, CO) and temperature. The isotopic signature of the graphite also reflects the specific mechanism that caused precipitation. The latter factor complicates the interpretation of isotopic data of fluid-deposited graphite, particularly when graphite precipitation was induced by the mixing of fluids (Valley and O'Neil, 1981; Kreulen and van Beek, 1983; Wada and Suzuki, 1983; Dunn and Valley, 1992; Kitchen and Valley, 1995).

The carbon source can be the same for some fluid-deposited graphite as for adjacent metamorphosed organic matter. The fluid that gives rise to a vein-type mineralization could have derived its carbon from the thermal maturation of local organic matter. Fluid-deposited graphite in which carbon probably has been derived totally from organic precursors ($\delta^{13}C$ values ranging from $-30.6$ to $-19$ permil in table 1) include those of Huelma and British Columbia (vein type), Borrowdale (replacement type), and Serranía de Ronda (table 1, entry #17), as well as the Water Hen intrusion in the Duluth Complex and portions of the Bushveld Complex (all dissemination types).

It is important to note that the organically derived carbon discussed here is inferred to have moved in a fluid phase that was derived from the devolatilization of heated organic matter. This model for the incorporation of biogenic carbon differs from those that involve the wholesale assimilation of organic sediments by an igneous melt (that is, "restitic" graphite; Kanaris-Sotiriou, 1997) or the physical mobilization in the solid state of pre-existing disseminated graphite (Erdosh, 1970). Mixing of fluids of "carbonate" and "organic" provenances also is possible, which can give rise to fluid-deposited graphite with intermediate isotopic signatures. Such mixed fluids appear to account for the formation of the vein mineralizations of south central New Hampshire (Rumble and Hoering, 1986) and perhaps for some of the disseminated graphite in the KTB drillcore (K. Bartels, J. Pasteris, J. Valley, unpublished data). The mixing and recycling of C-bearing fluids derived from organic and/or carbonate precursors also could occur in the deep crust or in the upper mantle, yielding – under appropriate conditions – a $CO_2$-rich fluid (Glassley, 1982). These $CO_2$-rich fluids could arguably have played a major role in the genesis of granulite-facies rocks (see discussions in Lamb and Valley, 1984, 1985) and in the formation of vein-type graphite mineralizations in Sri Lanka (Katz, 1987; Dissanayake, 1994) and India (Santosh and Wada, 1993).

Pearson, Boyd, and Nixon (1990) and Pearson and others (1994) studied fluid-deposited graphite of mantle origin in ultramafic xenoliths. This graphite has a $\delta^{13}C$ of $-12.3$ to $-3.8$ permil, which is close to that usually found in MORB rocks and diamonds. Processes that produce large isotopic fractionation of carbon, however, might lead to lighter values, as postulated by Pineau, Javoy, and Kornprobst (1987) for disseminated graphite in ultramafic xenoliths ($\delta^{13}C = -24.6$ to $-14.4$ permil). Schulze and others (1997) recently reported $\delta^{13}C$ values as light as $-14.31$ permil for graphite in mantle-derived eclogite xenoliths, which led them to consider that this graphite may be derived from subducted oceanic lithosphere. The fact that the fluid-deposited graphite from Sri Lanka is among the isotopically heaviest ($\delta^{13}C$ of $-7$ to $-9$ permil) of all the examples listed in table 1 supports the hypothesis of a mantle-derived carbon source.

Mixing of organic and mantle reservoirs is also possible: The isotopic signatures of graphite from the vein-type mineralizations associated with lherzolitic rocks from Beni-Bousera and the tectonically related Serranía de Ronda ($\delta^{13}C$ of $-18.0$ to $-16.5$ permil) are thought to be due to assimilation of organic carbon and subsequent mixing with mantle-derived C-bearing fluids (Luque, Rodas, and Galán, 1992). Similarly, the participation of $CO_2$-rich mantle fluids cannot be completely ruled out in the formation

of vein deposits in granulitic rocks (Dobner, Hahn-Weinheimer, and Hirner, 1981; Dissanayake, 1994). The fact that the mantle has a $\delta^{13}C$ signature between that of the organic and carbonate reservoirs leads to much of the ambiguity.

The above series of factors is largely responsible for the range of $\delta^{13}C$ values observed in fluid-deposited graphite (see examples in table 1), and it certainly complicates the interpretation of such data. However, a very important observation is that, regardless of the composition of the fluid and the mechanism of precipitation, isotopic exchange apparently does not occur readily once graphite is fully crystallized, due to the very sluggish diffusion kinetics of carbon in graphite whether of metamorphic or fluid-deposited origin (Chacko and others, 1991; Dunn and Valley, 1992; Scheele and Hoefs, 1992; Kitchen and Valley, 1995). This preservation of the isotopic signature, in principle, aids in the unraveling of the carbon source of metamorphic and fluid-deposited graphite. However, the isotopic interpretation of fluid-deposited graphite remains difficult due to the possibility of the mixing of different carbon reservoirs.

*The C–O–H system.*–Most igneous and metamorphic fluids are dominated by $H_2O$. Their compositions are represented well by the C-O-H system, which also provides a good model for the deposition of graphite from a fluid. This system can be represented graphically in a C-O-H ternary diagram (Holloway, 1984) that permits representation of the stability field of graphite (+ fluid) as a function of T, P, bulk composition, and $fO_2$ (fig. 5). As constrained by the phase rule, not all these parameters can be independent at once. For instance, at any specified T and P, there are only certain compositions of the fluid that can be in equilibrium with graphite, that is, those compositions along the "graphite saturation curve." It follows that at a specific T and P (1) each composition on the saturation curve represents a specific $fO_2$, and (2) for any given bulk composition within the field graphite + fluid, the system consists of graphite and a homogeneous C-O-H fluid.

These basic systematics allow one to consider not only the most fundamental chemical equilibria in the system, but also what chemical reactions and changes in intensive parameters are expected geologically to induce the precipitation of graphite. For instance, in figure 5 it should be noted that graphite can be in equilibrium with fluids of widely varying oxygen fugacities at a given T and P. Contrary to common perception, extremely reducing conditions are not required in order to stabilize and precipitate graphite. Furthermore, fluids in equilibrium with graphite can vary from anhydrous to those that are dominantly aqueous.

When elemental carbon is present as a solid phase at a fixed P-T condition, the C-O-H system becomes univariant, and the graphite-fluid equilibrium can be expressed in terms of the following four independent equations (French, 1966; Ohmoto and Kerrick, 1977; Frost, 1979; Holloway, 1984; Lamb and Valley, 1985):

$$C + O_2 = CO_2;\ C + \tfrac{1}{2}O_2 = CO;\ H_2 + \tfrac{1}{2}O_2 = H_2O;\ C + 2H_2 = CH_4.$$

At high temperature and relatively high oxygen fugacity, the fluid coexisting with graphite mainly consists of $H_2O$ and $CO_2$, and the equilibrium $C + O_2 = CO_2$ is the dominant control on the stability of graphite (Frost, 1979). At lower oxygen fugacity, $CH_4$ becomes the most important species, with $H_2O$ and $H_2$ as the other major components (Holloway, 1984; Jakobsson and Oskarsson, 1990; Cesare, 1995); at these conditions the controlling equilibrium is $C + 2H_2O = CH_4 + O_2$.

The size of the graphite stability field is a function of several geologically important parameters (fig. 5A and B). The graphite field is enlarged (and thus the carbon content of the coexisting fluid is reduced) as pressure is increased and/or as temperature is decreased (Ohmoto and Kerrick, 1977; Ferry and Baumgartner, 1987). In addition, the position of the graphite saturation curve is also a function of the degree of crystallinity of the solid carbon phase (fig. 5C). Compared to the saturation curve for well crystalline

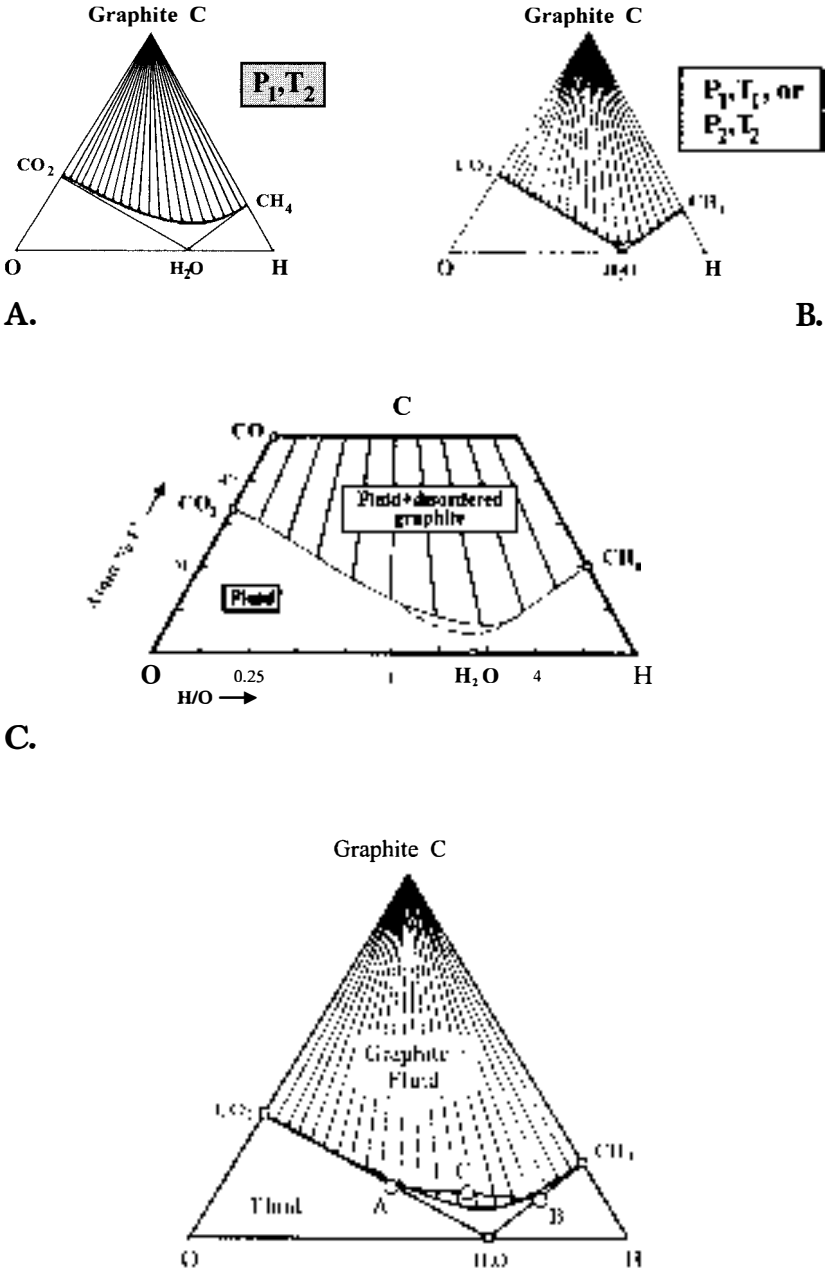


Fig. 5 (A) and (B). Composition triangles for the system C-O-H indicating the dependence of the graphite stability field on T and P. Upper portion of diagram shows field of graphite + fluid; tie lines connect graphite with equilibrium compositions of fluid. $T_1$ and $T_2$ represent two different temperatures, where $T_2 > T_1$; $P_1$ and $P_2$ are two different pressure conditions, where $P_2 > P_1$. (C) Diagrammatic composition of the C-O-H system at fixed P-T (400°C and 2 kb) showing that the size of the graphite stability field depends on the degree of crystallinity of graphite. Solid curve outlines field of stability of disordered graphite; dashed curve indicates well ordered graphite (from Ziegenbein and Johannes, 1980). Reprinted with permission of the authors. (D) Mixing of two carbon-bearing fluids in the composition triangle for the system C-O-H at 500°C, 1 kb. Fluid A is a $H_2O$-$CO_2$ mixture and fluid B is an aqueous, methane-rich fluid. Neither fluid A nor B is in equilibrium with graphite. On mixing, fluid C is produced, which precipitates graphite.

graphite, the curve for graphite that is not perfectly well crystalline (detailed discussions in later sections) shifts toward the carbon apex, thereby diminishing the "graphite" stability field (Ziegenbein and Johannes, 1990).

*The mechanisms of mobilization.*–Carbon is transported as mobile species such as $CH_4$ and $CO_2$ (released, for example, during thermal maturation of organic matter) dominantly in aqueous fluids, as demonstrated in the experimental work of Ziegenbein and Johannes (1980). Movement as carbonate and bicarbonate ions in aqueous solutions also provides a means of transporting carbon. Thus, certain molecular reactions must occur both to transport and ultimately to precipitate graphite. Among the geologically most important reactions that change the carbon content and speciation of a fluid and that may lead to the precipitation of graphite are fluid-rock interactions (mineral dissolution and precipitation), fluid mixing (changing the bulk carbon content of the fluid), and redox reactions (changing the carbon species that are stable). Reactions of the type $CO_2 + CH_4 = 2C + 2H_2O$ demonstrate how carbon is transferred from a homogeneous C-O-H fluid (mobile carbon) into a graphite-bearing (precipitated carbon) aqueous fluid, in other words, how carbon is transported via a gas phase and subsequently deposited as graphite elsewhere (Walther and Althaus, 1993). In a sense, the mobility of carbon-bearing fluids provides a means of "transporting graphite."

Combined geological and textural evidence can be used to obtain information about the flow of carbon-bearing fluids and whether the precipitation of graphite occurred in a single stage or as a consequence of successive generations of fluid reactions. These criteria can be used to distinguish between channelized fluids and more pervasive fluid flow as documented by Duke and Rumble (1986) for the New Hampshire graphite occurrences and by Bartels and Pasteris (1994) for graphite within the rocks drilled by the KTB continental deep drill hole in Germany. Reactions along the fluid path can change the composition of the fluid and its speciation (Lamb and Valley, 1985; Ferry and Baumgartner, 1987), which complicate the isotopic interpretation of the final graphite precipitates, and can lead to isotopic zoning.

Tectonically weakened zones are favorable for fluid infiltration, since they offer migration channels for C-O-H fluids. This effect would explain why graphite concentrations are common in shear zones (Ziegenbein and others, 1989; Bartels and Pasteris, 1993; Large, Christy, and Fallick, 1994). In addition, the fluid pressure can promote hydraulic fracturing, favoring the formation of epigenetic graphite veins (Katz, 1987; Luque, Rodas, and Galán, 1992; Dissanayake, 1994).

## *Mechanisms of Precipitation*

The chemical systematics of the C-O-H system indicate that the precipitation of solid carbon from fluids can be achieved by several means involving either isochemical P-T changes or isobaric-isothermal changes in chemistry. The thermodynamic requirement for graphite precipitation is that P-T conditions change so the graphite saturation surface moves over the fluid bulk composition (fig. 5).

*Isobaric cooling or isothermal pressure increase.*–Precipitation of graphite in the C-O-H system can be induced isochemically by a decrease in temperature and/or an increase in pressure, because the graphite stability field increases in size (and the carbon content of the coexisting fluid decreases) following either of those changes (Ohmoto and Kerrick, 1977; Frost, 1979; Ziegenbein and others, 1989; fig. 5A and B). Cooling of a C-bearing fluid is probably the most effective mechanism to cause graphite precipitation (Dubessy, 1984; Mathez and others, 1989). For instance, heated C-O-H fluids deep in the crust (or even in the upper mantle) could rise up and away from their heat source, cool, and then precipitate carbon. This process appears to be an efficient means to transport and (re-)deposit carbon over a wide range of temperature: It has been invoked to explain the presence of graphite in epithermal systems (T = 100°–300°C) (Reed and Spycher, 1985) and in ultramafic mantle xenoliths from depths on the order of 60 to 90 km and at temperatures of 600° to 1000°C (Pearson and others, 1994).

The above discussion applies to C-O-H fluids in general. In metamorphic terranes, such fluids coexist with only solid phases. A C-O-H fluid also can exsolve from a magma as it cools and fractionates, but before it reaches the solidus. Cooling of this fluid can induce massive precipitation of graphite, which in turn causes major changes in the composition of the remaining fluid (Mathez and others, 1989).

*Hydration reactions.*–There are several mechanisms for graphite precipitation that involve changing the composition of the fluid in order to bring the system into the field of graphite stability at some P and T. For instance, under isobaric-isothermal conditions, hydration reactions can deplete a fluid in $H_2O$, thereby enriching it in carbon causing graphite precipitation (Rumble, Duke, and Hoering, 1986; Stevens, 1997). This relation may explain the common occurrence of hydrated minerals (such as chlorite and smectite) directly intergrown with graphite or present in the host rocks (Borrowdale, Huelma, Fish Lake, and Water Hen intrusions in the Duluth Complex, KTB metabasites). In contrast, an isobaric-isothermal decrease in the $CO_2$ content of a fluid could dissolve graphite, because it would deplete the fluid of carbon. This is probably one reason that calcite and other carbonate minerals so rarely occur with fluid-deposited graphite.

*Changes in the ambient oxygen fugacity conditions.*–As mentioned above, extremely reducing conditions are not needed to cause the precipitation of graphite from a C-O-H fluid. In fact, carbon can precipitate due to either an oxidation or a reduction process (Frost, 1979). For instance, recent hypotheses on vein-type graphite in granulite-facies terranes (Sri Lanka, India) suggest that graphite precipitated when $CO_2$-rich fluids infiltrated low-$fO_2$ rocks (graphitic gneisses) and underwent reduction (Santosh and Wada, 1993; Dissanayake, 1994). Another example of this mechanism of precipitation is shale-hosted graphite that appears to have formed as $CO_2$-rich fluids infiltrated from adjacent carbonates and were reduced during their passage through the shales (Baker, 1988; Connolly and Cesare, 1993). In contrast, introduction of a low-$fO_2$, methane-rich fluid into a fracture system will induce a gradient in $fO_2$ between the walls of the fractures and the fluid. If the fluid composition changes in response to diffusion, graphite can precipitate due to oxidation, as proposed by Frost (1979) to explain the origin of graphite vein deposits.

*Mixing of different C-bearing fluids.*–Changes in fluid composition also can be achieved by *in situ* diffusional introduction of one gas species into another or by more dynamic fluid mixing between two chemically distinct reservoirs. The reduction of $CO_2$ by addition of $H_2$ in hydrothermal fluids is considered by Mastalerz, Bustin, and Sinclair (1995) as a likely precipitation mechanism for poorly ordered graphite in the Erickson hydrothermal system. This mechanism was monitored experimentally at 725°C by Pasteris and Chou (1998), who induced $H_2$ to diffuse into natural pure $CO_2$ inclusions in quartz, causing the precipitation of disordered graphite. Hydrogen diffusion into inclusions has been inferred to occur in nature under specific metamorphic conditions (Hall and Bodnar, 1990; Hall, Bodnar, and Craig, 1991). The effects of fluid mixing on the precipitation of graphite can be visualized on the C-O-H diagram (fig. 5D). The mixing of two aqueous fluids (which are not saturated with respect to graphite), one $CO_2$-rich (A) and another $CH_4$-rich (B), can result in an intermediate composition (C) within the field graphite + fluid (Rumble and Hoering, 1986; fig. 5D). In this situation, precipitation of graphite will take place by the reaction $CO_2 + CH_4 = 2C + 2H_2O$.

*Precipitation reactions catalyzed by reducing agents.*–In a relatively small number of cases, graphite precipitation may be induced by the presence of catalyzing minerals. It is well known that certain compounds (especially sulfides and oxides) act as catalysts during the process of metamorphic graphitization (Grew, 1974; Bonijoly, Oberlin, and Oberlin, 1982). The influence of such catalysts in the formation of graphite from fluids has been documented both experimentally (Morgan, Chou, and Pasteris, 1992) and in

some natural occurrences. Among the sulfides, pyrrhotite appears to play a role in the graphite vein deposits of New Hampshire (Duke and Rumble, 1986). The presence of graphite rims around pyrite and hematite cores led Strens (1965) to postulate that graphite precipitation was catalyzed by these minerals at the Borrowdale replacement deposit. Stibnite and other Fe-Ni-Cu sulfoantimonides also appear to influence the precipitation of graphite in hydrothermal vents (Jedwab and Boulegue, 1984). Sulfide-oxide spherules have been proposed to catalyze graphite formation in vesicles of submarine basalts (Mathez and Delaney, 1981). It is possible that once the catalytic reaction has been initiated, graphite deposition continues by homogeneous nucleation (Mathez and Delaney, 1981). Textural evidence for homogeneous nucleation in fluid-deposited graphite was found by Duke and Rumble (1986) who reported the nucleation of radially oriented spherulites on graphite flakes.

## DISCUSSION

*Degree of crystallinity.*–There is more involved in the deposition of graphite from a geological fluid than is addressed in the simplified models and mechanisms discussed above. In most of the latter discussions, it was assumed that the precipitate is well-ordered, fully crystalline, pure-carbon graphite. Even though this is true for most fluid-deposited graphite that has been recognized and studied so far, such assumptions are not universally true. The thermochemical properties of "disordered" graphite are different from those of well-crystalline graphite (Ziegenbein and Johannes, 1980). Ziegenbein and Johannes (1990) have pointed out that there is a displacement in the graphite saturation curve in the case of poorly ordered graphite (see fig. 5C), which also results in a change in the composition of the fluid coexisting with graphite.

The structural data obtained by means of XRD, Raman spectroscopy, and HRTEM indicate that natural graphite precipitated from fluids is fairly homogeneous (unlike metamorphic graphite), that is, there are no large fluctuations in the "crystallinity" of a given sample. In addition, the majority of natural fluid-deposited graphite samples are characterized by very high crystallinity. Since poorly crystalline (disordered) graphite can be brought to saturation in laboratory experiments involving a C-O-H fluid (Ziegenbein and Johannes, 1980; Pasteris and Wanamaker, 1988; J. Krautheim, ms; Wopenka and Pasteris, 1993; Morgan and others, 1993; Pasteris and Chou, 1998; see fig. 4), the very limited number of known natural occurrences of "disordered" fluid-deposited graphite is surprising (Pasteris and Luque, 1997), but it has been reported, for instance in shear zones in the KTB borehole (see fig. 4; Reutel and others, 1989; Bartels and Pasteris, 1994) and in veins in the Erickson hydrothermal system (Mastalerz, Bustin, and Sinclair, 1995).

*Kinetics of precipitation.*–Since fluid deposition of graphite clearly involves both nucleation and grain growth, one also must consider how kinetics might affect the precipitation conditions and the physical properties of fluid-deposited graphite. Ziegenbein and Johannes (1980) showed that graphite-fluid equilibration can be very sluggish below about 700°C. Graphite does not always precipitate within its stability field, and the solid carbon phase that first precipitates may not be the stable form.

The compositional stability field for disordered graphite is smaller than that for ordered graphite (fig. 5C), which suggests that ordered graphite might be stabilized more readily than disordered graphite. However, structurally disordered graphite is the phase that first precipitates in many experiments (Ziegenbein and Johannes, 1990; G. Krautheim, ms; Pasteris and Chou, 1998). It is possible that disordered graphite is easier to nucleate at low temperatures than is ordered graphite, but that at some threshold temperature the larger size of the stability field for ordered graphite becomes the controlling factor. The fact that the rhombohedral polytype of graphite occurs in abundances up to 32 wt percent in the Borrowdale (England) and up to 25 wt percent in the Huelma (Spain) volcanic-hosted deposits (Kwiecinska, 1980; Barrenechea and others, 1997; respectively)

suggests that there also may be important kinetic controls on the polytype that initially nucleates. As discussed by Barrenechea and others (1997), the metastable rhombohedral graphite phase may be preserved in the above two deposits due to the high cooling rate associated with volcanic environments.

*Question of geothermometry.*–The fact that fluid-deposited graphite, just like metamorphic graphite, can exist in disordered forms suggests the possibility of investigating the physical properties of fluid-deposited graphite as an aid to deciphering the mechanism of its precipitation. Such an approach requires high-quality analytical data on many fluid-deposited graphite occurrences, including some whose conditions of formation are well understood. As already noted, most natural fluid-deposited graphite occurrences are homogeneous in crystallinity. This suggests that certain physical parameters could be used for evaluating the temperature at which the graphite precipitated, that is, in analogy with geothermometric estimates for metamorphic graphite (Landis, 1971; Grew, 1974; Shengelia, Akhvlediani, and Ketskhoveli, 1979; Beny-Bassez and Rouzaud, 1985; Wopenka and Pasteris, 1993; Wada and others, 1994). However, the reliability of metamorphic graphite geothermometry is still debated, since the effects of pressure, shearing, organic precursor, and host lithology affect the process of graphitization.

Similarly, it remains difficult to evaluate the effects on the physical properties of graphite of individual fluid-depositional parameters, such as pressure, temperature, and oxygen/hydrogen fugacity. Firstly, reliance on natural samples does not permit selection of those variables independently. Secondly, we have only estimates of the values of those intensive parameters. Fluid-deposited graphite of the Erickson hydrothermal system (Mastalerz, Bustin, and Sinclair, 1995) is considered to have formed at about 300°C (based on vitrinite reflectance and fluid-inclusion data), a temperature in keeping with the very disordered structure of this graphite. Thermal studies carried out on the KTB graphite in the current work, however, gave significantly higher temperatures for the graphite's differential-thermal-analysis maximum (665°C) than those obtained from geothermometric calculations on coexisting minerals (T = 300°–400°C; Skrotzki and Reutel, 1990; Bartels and Pasteris, 1993; Walther and Althaus, 1993). One reason for the disparity in recorded temperatures between graphite and coexisting silicates may be that graphite's crystallinity does not retrograde during cooling, whereas silicates may continue their elemental diffusion as temperature drops. Moreover, consistent variation of graphite crystallinity with temperature does not assure that the precipitation was an equilibrium process. The effect of kinetics on the crystallinity of fluid-deposited graphite must be considered. With the exception of the KTB and Erickson occurrences, documented fluid-deposited graphite mineralizations appear to be restricted to recognized high-temperature environments (see table 1) or at least show high degrees of crystallinity. However, the database on confirmed fluid-deposited graphite is still small, and few experimental studies on fluid-deposition of graphite provide the necessary structural analyses. We therefore encourage researchers to do more structural analyses on natural fluid-deposited graphite and additional experiments in which the graphite precipitates are characterized in detail.

The lack of documentation on natural fluid-deposited graphite compels us to use results from laboratory experiments on deposition of graphite from a fluid under controlled conditions of pressure, temperature, and $fO_2$ (or $fH_2$). J. Krautheim's (ms) and G. Krautheim's (ms) work demonstrated that the crystallinity of graphite was enhanced by increases in pressure, temperature, and/or $fO_2$ (decrease in $fH_2$). The same fugacity control is inferred from the analyses and observations of Grew (1974), Wintsch and others (1981), Wopenka and Pasteris (1993), and Wada and others (1994), who recognized that *organic matter* metamorphosed at a certain temperature in carbonate rocks was more highly crystalline than that in pelitic rocks at the same temperature. Pasteris and Chou (1998) also showed that for fluids that undergo compositional change in order to

bring them to graphite saturation, the graphite crystallinity is controlled by the $fH_2$ that pertained when saturation *initially* was attained.

The specific temperature control on graphite crystallinity remains problematic. Experiments on the fluid-deposition of graphite (Pasteris and Wanamaker, 1988; J. Krautheim, ms; G. Krautheim, ms) indicate that crystallinity increases with increasing run duration (up to several days or weeks, depending on temperature; then crystallinity remains constant). However, even synthetic precipitates formed at 900°C, 15 kb are not as well crystalline as most natural fluid-deposited graphite. Unfortunately, however, these results cannot be extrapolated to geologic time scales.

*Similarities between metamorphic and fluid-deposited graphite.*–A question of interest is whether two natural graphite samples formed at the same temperature would have the same properties, if one were deposited from a fluid and the other were metamorphosed organic matter. Due to the lack of confirmed temperatures for the formation of fluid-deposited graphite, this question cannot be answered. However, one can investigate the co-variation in different structural parameters of graphite to compare the development of crystallinity in metamorphic versus fluid-deposited graphite. For comparative purposes, DTA temperatures can be used in the absence of formation temperatures. There are some striking contrasts in the relations between structural parameters and DTA maxima for these two types of graphite. Kwiecinska's (1980) plot (fig. 6) of the measured $d_{(002)}$ versus DTA maxima for about 30 samples of (dominantly) metamorphic and (minor) fluid-deposited graphite shows a strong linear correlation. The superposition of our data for eight fluid-deposited graphite samples listed in table 1 (entries 1, 2, 6, 8, 10, 12, 17, and 18) onto Kwiecinska's (1980) diagram shows that for a given DTA temperature, the degree of crystallinity of six of our fluid-deposited graphite samples is significantly higher than that for the average (metamorphic) graphite. In other words, for a given degree of crystallinity (value of $d_{(002)}$), most of our fluid-deposited graphite samples show lower DTA temperatures than do metamorphic graphite samples (fig. 6).

This finding contrasts with those of Pasteris and Wanamaker (1988), J. Krautheim (ms), and Pasteris and Chou (1998), whose experiments showed that considerably higher temperatures would be needed to produce fully crystalline graphite by experimental fluid-deposition than by natural metamorphism of organic matter. The present comparison unfortunately suffers from the dissimilarity between the conditions of pressure and length of time in the experiments and those in natural settings. An additional complexity is revealed by the experiments of J. Krautheim (ms) and Pasteris and Chou (1998), which demonstrate that the degree of crystallinity of fluid-deposited graphite is strongly affected by the $fH_2$ of the fluid from which it precipitates.

From a simply experimental viewpoint, it thus would appear that one should not expect close correlation between the degree of crystallinity of fluid-deposited graphite and its temperature of formation. However, in nature, unlike in the experimental laboratory, not all combinations of gas fugacities are equally probable. Certain temperature-gas fugacity pathways are favored geologically due to fluid-mineral equilibria (including mineral-buffering and fluid immiscibility). Such interrelationships suggest that useful correlations can be found between the degree of crystallinity of fluid-deposited graphite and its formation temperatures if appropriate indicators of gas fugacity can be identified. Previous work by Luque, Barrenechea, and Rodas (1993) supports such crystallinity-temperature relations in natural samples. Additional similarities and differences between metamorphic and fluid-deposited graphite occurrences are listed in table 2.

In summary, there are several important geologic, geochemical, and petrologic consequences of the fluid deposition of graphite. The attainment of graphite saturation in a fluid decreases the degrees of freedom of the system by one and may cause $fO_2$-buffering (that is, control on composition) in the fluid. Moreover, in a fluid-dominated igneous or metamorphic environment, graphite saturation can control the T-$fO_2$ evolu-

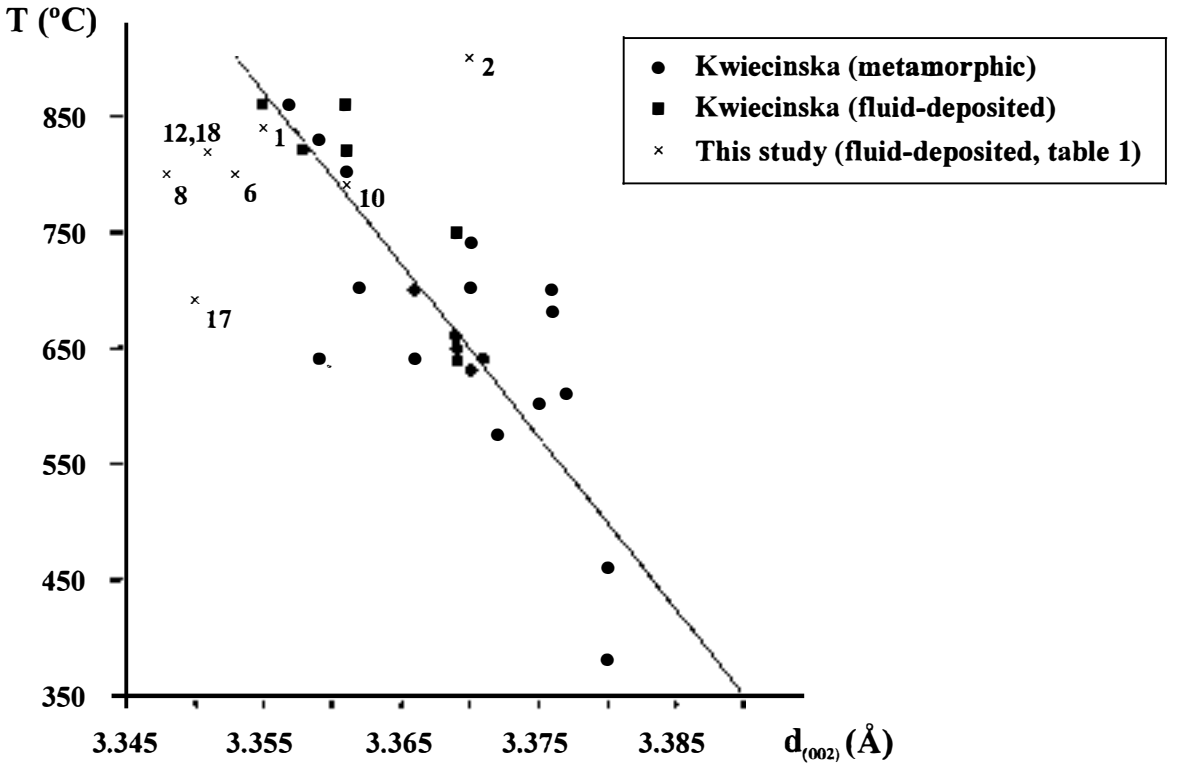


Fig. 6. Relation between the DTA maximum temperatures (exothermic peaks) and the interlayer $d_{002}$ spacings for both metamorphic and fluid-deposited graphite (modified from Kwiecinska, 1980, fig. 13). Kwiecinska's original data points shown as filled circles for metamorphic graphite and as filled squares for those occurrences that we infer to represent fluid-deposited graphite; correlation line as drawn by Kwiecinska. X-symbols represent fluid-deposited graphite occurrences from table 1 (keyed to entry numbers in table).

TABLE 2

*Differences between metamorphic and fluid-deposited graphite*

| Characteristic | Metamorphic graphite | Fluid-deposited graphite |
|---|---|---|
| Crystallite size versus grain size | Macroscopic grain size increases as crystallite (unit of crystallographic continuity) size increases | Macroscopically fine-grained (described as "amorphous lumps" commercially) graphite can show maximum degree of crystallinity. Example: Water Hen Intrusion, figure 4. |
| Homogeneity of crystallites revealed by HRTEM | Even in high-grade metamorphic rocks, some graphite grains are poorly ordered. See examples in Leger and others (1996) and Buseck and Huang (1985). | Fluid-deposited graphite is homogeneous at grain-to-grain scale. Example: Betic Cordillera (this work). |
| Range in crystallinity | Carbonaceous matter ranges from poorly ordered kerogens to graphite with maximum crystallinity. See examples in Grew (1974) and Wopenka and Pasteris (1993). | With only a few recorded exceptions (a hydrothermal system; in fluid inclusions), natural fluid-deposited graphite concentrations are of very high crystallinity. Examples throughout this paper. |
| Temperature versus crystallinity | Linear correlation between DTA temperature maximum and XRD d(002). Example: Kwiecinska, 1980 (our figure 6). | Several fluid-deposited graphites lie to the high-crystallinity side of this linear correlation. See figure 6. |

tion of the entire system as it cools (see discussions in Ballhaus and Stumpfl, 1985, and in Mathez and others, 1989). Such buffering will affect oxidation-dependent equilibria in the coexisting fluid, melt, and/or rock, such as those controlling the aqueous complexes responsible for mobilizing metals, and the $Fe^{2+}/Fe^{3+}$ ratios that control the mineralogy of the iron-bearing phases that form. The thermodynamics of the C-O-H system also allow for abrupt changeovers – under normal geologic variations in conditions in the crust and mantle – from conditions of carbon-mobilization to those of carbon-deposition. In other words, in dynamic geologic systems, the P-T-$fO_2$ controls on graphite saturation allow for the fluid-scavenging of carbon from large volumes of rock with the subsequent deposition of this carbon in much more concentrated deposits elsewhere. In this way, carbon becomes localized in certain regions of the crust and mantle over time (see Haggerty, 1986, concerning mantle carbon). When carbonic fluids move through fracture systems in the crust and mantle, graphite precipitation can seal these fractures to further fluid movement. In these ways, fluid deposition of graphite is a major factor in the terrestrial carbon mass balance.

In conclusion, there is still much to be learned about the different types of fluid-deposited graphite, the mechanisms of deposition, and the effects of the formational mechanism on the properties of graphite precipitates. As demonstrated by the examples in this paper, the chemical and physical characteristics of such fluid-deposited graphite help to specify its mechanism of deposition and, to some degree, distinguish fluid-deposited from metamorphic graphite. For example, carbon isotope ratios help constrain the source of the carbon, whereas the measured degree of crystallinity helps to constrain the range of temperatures and gas fugacities over which deposition occurred. Compared to metamorphic graphite, fluid-deposited graphite appears to be dominated by a high degree of crystallinity and marked homogeneity of crystallinity. Fluid-deposited graphite shows greater isotopic zoning, however. In addition, the temperature-crystallinity relations of fluid-deposited graphite are more complex than those of metamorphic graphite.

ACKNOWLEDGMENTS

This work has been partially supported by the Spanish DGICYT through Project PB93-0064 and also by National Science Foundation grants EAR 91-16967 and EAR 94-17677 to JDP. We thank the following people for providing graphite samples: I-Ming

Chou, Henk Dahlberg, Edward Duke, and Brian Young. We thank Karen Bartels and John Valley for providing previously unpublished data. This paper has benefitted from reviews by Steve Dunn, John Holloway, and John Valley.

## References

Acharya, B. C., and Dash, B., 1984, Graphite in Eastern Ghats Precambrian migmaties, Orissa, India: Transactions, Royal Society of Edinburgh, Earth Science, v. 75, p. 391–406.

Arneth, J. D., Schidlowski, M., Sarbas, B., Goerg, U., and Amstutz, G. C., 1985, Graphite content and isotopic fractionation between calcite-graphite pairs in metasediments from the Mgama Hills, Southern Kenya: Geochimica et Cosmochimica Acta, v. 49, p. 1553–1560.

Baker, A. J., 1988, Stable isotope evidence for limited fluid infiltration of deep crustal rocks from the Ivrea Zone, Italy: Geology, v. 16, p. 492–495.

Ballhaus, C. G., and Stumpfl, E. F., 1985, Occurrence and petrological significance of graphite in the Upper Critical Zone, western Bushveld Complex, South Africa: Earth and Planetary Science Letters, v. 74, p. 58–68.

Barrenechea, J. F., Luque, F. J., Rodas, M., and Pasteris, J. D., 1997, Vein-type graphite in the Jurassic volcanic rocks of the external zone of the Betic Cordillera (Southern Spain): Canadian Mineralogist, v. 35, p. 1379–1390.

Bartels, K. S., and Pasteris, J. D., 1993, Preliminary results on the relation between graphite derived from metamorphosed organic matter and fluid deposition in rocks of the KTB-VB and -HB: A Raman spectroscopic study, *in* Emmermann, R., Lauterjung, J., and Umsonst, T., editors, Kontinentales Tief ohr-programm der Bundesrepublik Deutschland, Report 93-2: Hannover, Germany, Niedersächsisches Landesamt für Bodenforschung, p. 499–502.

—— 1994, Multiple generations of fluid deposited graphite in rocks from the KTB: Geological Society of America Abstracts with Programs, p. A-223.

Beny-Bassez, C., and Rouzaud, J. N., 1985, Characterization of carbonaceous materials by correlated electron optical microscopy and Raman microspectroscopy: Scanning Electron Microscopy v. 1985, p. 119–132.

Benoist, M., Oberlin, M., and Oberlin, A., 1982, A possible mechanism for natural graphite for ation: International Journal of Coal Geology, v. 1, p. 283–317.

Buseck, P. R., and Huang, B. J., 1985, Conversion of carbonaceous material to graphite during metamorphism: Geochimica et Cosmochimica Acta, v. 49, p. 2003–2016.

Cameron, E. N., and Weis, P. L., 1960, Strategic graphite: A survey: United States Geological Survey Bulletin, v. 1082-E, p. 201–321.

Cesare, B., 1995, Graphite precipitation in C-O-H fluid inclusions: closed system compositional and density changes, and thermobarometric implications: Contributions to Mineralogy and Petrology, v. 122, p. 62–71.

Chacko, T., Mayeda, T. K., Clayton, R. N., and Goldsmith, J. R., 1991, Oxygen and carbon isotope fractionations between $CO_2$ and calcite: Geochimica et Cosmochimica Acta, v. 55, p. 2867–2882.

Connolly, J. A. D., and Cesare, B., 1993, C-O-H fluid composition and oxygen fugacity in graphitic metapelites: Journal of Metamorphic Geology, v. 11, p. 379–388.

Davies, G. R., Nixon, P. H., Pearson, D. G., and Obata, M., 1993, Tectonic implications of graphitized diamonds from the Ronda peridotite massif, southern Spain: Geology, v. 21, p. 471–474.

Des Marais, D. J., and Moore, J. G., 1984, Carbon and its isotopes in mid-oceanic basaltic glasses: Earth and Planetary Science Letters, v. 69, p. 43–57.

Diessel, C. F. K., Brothers, R. N., and Black, P. M., 1978, Coalification and graphitization in high-pressure schists in New Caledonia: Contributions to Mineralogy and Petrology, v. 68, p. 63–78.

Diessel, C. F. K., and Offler, R., 1975, Change in physical properties of coalified and graphitised phytoclasts with grade of metamorphism: Neues Jahrbuch für Mineralogie Monatshefte, v. 1, p. 11–27.

Diessel, C. B., 1981, The origin of graphite of Sri Lanka: Organic Geochemistry, v. 3, p. 1–7.

—— 1994, Origin of vein graphite in high-grade metamorphic terranes. Role of organic matter and sediment subduction: Mineralium Deposita, v. 29, p. 57–67.

Dobner, A., Graf, W., Hahn-Weinheimer, P., and Hirner, A., 1978, Stable carbon isotopes of graphite from Bogala Mine, Sri Lanka: Lithos, v. 11, p. 251–255.

Duba, A. G., and Shankland, T. J., 1982, Free carbon and electrical conductivity in the Earth's mantle: Geophysical Research Letters, v. 9, p. 1171–1174.

Dubessy, J., 1984, Simulation of chemical equilibria in the C-O-H system, methodological consequences for fluid inclusions (in French): Bulletin de Mineralogie, v. 107, p. 155–168.

Duke, E. F., Galbreath, K. C., and Trusty, K. J., 1990, Fluid inclusion and carbon isotope studies of quartz-graphite veins, Black Hills, South Dakota, and Ruby Range, Montana: Geochimica et Cosmochimica Acta, v. 54, p. 683–698.

Duke, E. F., and Rumble III, D., 1986, Textural and isotopic variations in graphite from plutonic rocks, South Central New Hampshire: Contributions to Mineralogy and Petrology, v. 94, p. 409–419.

Dunn, S. R., and Valley, J. W., 1992, Calcite-graphite isotope geothermometry: a test for polymetamorphism in marble, Tudor gabbro aureole, Ontario, Canada: Journal of Metamorphic Geology, v. 10, p. 487–501.

Erdosh, G., 1970, Geology of Bogala mine, Ceylon and the origin of vein-type graphite: Mineralium Deposita, v. 5, p. 375–382.

—— 1979, Abiotic carbon and the formation of graphite deposits: Economic Geology, v. 67, p. 383–385.

Ferry, J. M., and Baumgartner, L., 1987, Thermodynamic models of molecular fluids at the elevated pressures and temperatures of crustal metamorphism, *in* Carmichael, I. S. E., and Eugster, H. P., editors, Thermodynamic Modeling of Geological Materials: Minerals, Fluids and Melts: Reviews in Mineralogy, v. 17, p. 323–365.

Ford, R. B., 1954, Occurrence and origin of the graphite deposits near Dillon, Montana: Economic Geology, v. 49, p. 31–43.
French, B. M., 1966, Some geological implications of equilibrium between graphite and a C-O-H gas phase at high temperatures and pressures: Reviews in Geophysics, v. 4, p. 223–253.
Frost, B. R., 1979, Mineral equilibria involving mixed-volatiles in a C-O-H fluid phase. The stabilities of graphite and siderite: American Journal of Science, v. 279, p. 1033–1059.
Frost, B. R., Fyfe, W. S., Tazaki, K., and Chan, T., 1989, Grain boundary graphite in rocks and implications for higher crustal conductivity in the lower crust: Nature, v. 340, p. 134–136.
Gervilla, F., ms, 1989, Mineralizaciones magmáticas ligadas a la evolución de las rocas ultramáficas de la Serranía de Ronda (Málaga, España): Ph.D. thesis, Universidad de Granada. 189 pp.
Gervilla, F., and Leblanc, M., 1990, Magmatic ores in high temperature alpine-type lherzolite massifs (Ronda, Spain, and Beni Bousera, Morocco): Economic Geology, v. 85, p. 112–132.
Glassley, W., 1982, Fluid evolution and graphite genesis in the deep continental crust: Nature, v. 295, p. 229–231.
Goossens, P. J., 1982, Graphite deposits of the Precambrian and their mining development, *in* The Development Potential of Precambrian Mineral Deposits: Oxford, United Kingdom, Pergamon Press, p. 123–134.
Grew, E. S., 1974, Carbonaceous material in some metamorphic rocks of New England and other areas: Journal of Geology, v. 82, p. 50–73.
Guilhaumou, N., Santos, M., Touray, J. C., Beny, C., and Dardenne, M., 1990, Multiphase methane-rich fluid inclusions in gold bearing quartz as illustrated at Pontal (Goias, Brazil): Mineralogical Magazine, v. 54, p. 257–261.
Haggerty, S. E., 1986, Diamond genesis in a multiply-constrained model: Nature, v. 320, p. 34–38.
Hahn-Weinheimer, P., and Hirner, A., 1981, Isotopic evidence for the origin of graphite: Geochemical Journal, v. 15, p. 9–15.
Hall, D. L., and Bodnar, R. J., 1990, Methane in fluid inclusions from granulites: a product of hydrogen diffusion?: Geochemica et Cosmochimica Acta, v. 54, p. 641–652.
Hall, D. L., Bodnar, R. J., and Craig, J. R., 1991, Evidence for postentrapment diffusion of hydrogen into peak metamorphic fluid inclusions from the massive sulfide deposits at Ducktown, Tennessee: American Mineralogist, v. 76, p. 1344–1355.
Hoefs, J., and Frey, M. J., 1976, The isotopic composition of carbonaceous matter in a metamorphic profile of the Swiss Alps: Geochimica et Cosmochimica Acta, v. 40, p. 945–951.
Hollister, V. F., 1980, Origin of graphite in the Duluth Complex: Economic Geology, v. 75, p. 764–766.
Holloway, J. R., 1984, Graphite-$CH_4$-$H_2O$-$CO_2$ equilibria at low-grade metamorphic conditions: Geology, v. 12, p. 455–458.
Huvelin, P., and Permingeat, F., 1980, Graphite, *in* Geologie des Gites Minéraux Marocains: Notes et Mémoires, Service Géologique du Maroc, v. 276 (1), p. 215–250.
Itaya, T., 1981, Carbonaceous material in pelitic schists of the Sanbagawa metamorphic belt in central Shikoku, Japan: Lithos, v. 14, p. 215–224.
Jakobsson, S., and Oskarsson, N., 1990, Experimental determination of fluid compositions in the system C-O-H at high P and T and low $fO_2$: Geochimica et Cosmochimica Acta, v. 54, p. 355–362.
Jedwab, J., and Boudouma, J., 1984, Graphite crystals in hydrothermal vents: Nature, v. 310, p. 41–43.
Jödicke, H., 1992, Water and graphite in the Earth's crust–an approach to interpretation of conductivity models: Surveys in Geophysics, v. 13, p. 381–407.
Kanaris-Sotiriou, R., 1997, Graphite-bearing peraluminous dacites from the Erlend volcanic complex, Faeroe-Shetland Basin, North Atlantic: Mineralogical Magazine, v. 61, p. 175–184.
Katz, M. B., 1987, Graphite deposits of Sri Lanka: a consequence of granulite facies metamorphism: Mineralium Deposita, v. 22, p. 18–25.
Kitchen, N. E., and Valley, J. W., 1995, Carbon isotope thermometry in marbles of the Adirondack Mountains, New York: Journal of Metamorphic Geology, v. 13, 577–594.
Klemd, R., Bröcker, M., and Schramm, J., 1995, Characterization of amphibolite-facies fluids of Variscan eclogites from the Orlica-Snieznik dome (Sudetes, SW Poland): Chemical Geology, v. 119, p. 101–113.
Krautheim, G., ms, 1993, Kristallinitätsbestimmungen an den Schichtmineralen Illit und Graphit: Ph.D. thesis, Universität Hannover, Germany, 113 p.
Krautheim, J., ms, 1993, Experimentelle Untersuchungen und thermodynamische Berechnungen zur Charakterisierung von Fluiden der unteren Erdkruste und des oberen Erdmantels: Ph.D. thesis, Universität Hannover, Germany, 83 p.
Kreulen, R., and Van Beek, P. C. J. M., 1983, The calcite-graphite isotope thermometer: data on graphite bearing marbles from Naxos, Greece: Geochimica et Cosmochimica Acta, v. 47, p. 1527–1530.
Kwiecinska, B., 1980, Mineralogy of natural graphites: Polska Akademi Nauk, Prace Mineralogiczne, v. 67, p. 1–79.
Lamb, W. M., and Valley, J. W., 1984, Metamorphism of reduced granulites in low $CO_2$ vapour free environment: Nature, v. 312, p. 56–58.
—— 1985, C-O-H fluid calculations and granulite genesis, *in* Tobi, A. C., and Touret, J. L., editors, The Deep Proterozoic Crust in the North Atlantic Provinces: Dordrecht, D. Reidel Publisher, p. 119–131.
Landis, C. A., 1971, Graphitization of dispersed carbonaceous material in metamorphic rocks: Contributions to Mineralogy and Petrology, v. 30, p. 34–45.
Large, D. J., Christy, A. G., and Fallick, A. E., 1994, Poorly crystalline carbonaceous matter in high grade metasediments: implications for graphitisation and metamorphic fluid compositions: Contributions to Mineralogy and Petrology, v. 116, p. 108–116.
Luque, F. J., ms, 1990, Contribución al conocimiento de las mineralizaciones de grafito asociadas a las rocas ultramáficas de la provincia de Málaga: Ph.D. thesis, Servicio de Publicaciones de la Universidad Complutense de Madrid, 293 p.

Luque, F.J., Barrenechea, J. F., Rodas, M., 1993, Graphite geothermometry in low and high temperature regimes: two case studies: Geological Magazine, v. 130, p. 501–511.
—— 1994, Volcanic-hosted graphite mineralization in the external parts of the Betic Cordilleras (Southern Spain): International Mineralogical Association 16th General Meeting Proceedings, p. 252–253.
Luque, F.J., Rodas, M., and Galán, E., 1992, Graphite vein mineralization in the ultramafic rocks of southern Spain: Mineralogy and genetic relationships: Mineralium Deposita, v. 27, p. 226–233.
Luque, F.J., Rodas, M., Velasco, F., and Galán, E., 1987, Mineralogía y geotermometría de los diques ácidos con grafito asociados a rocas ultramáficas de la Serranía de Ronda, Málaga: Estudios Geológicos, v. 43, p. 367–375.
Mainwaring, P. R., and Naldrett, A. J., 1977, Country-rock assimilation and the genesis of Cu-Ni sulfides in the Water Hen intrusion, Dulut Complex, Minnesota: Economic Geology, v. 72, p. 1269–1284.
Mastalerz, M., Bustin, R. M., and Sinclair, A. J., 1995, Carbon-rich material in the Erickson hydrothermal system, northern British Columbia, Canada: Origin and formation mechanisms: Economic Geology, v. 90, p. 938–947.
Mathez, E. A., 1987, Carbonaceous matter in mantle xenoliths: Composition and relevance to the isotopes: Geochimica et Cosmochimica Acta, v. 51, p. 2339–2347.
Mathez, E. A., and Delaney, J. R., 1981, The nature and distribution of carbon in submarine basalts and peridotite nodules: Earth and Planetary Science Letters, v. 56, p. 217–232.
Mathez, E. A., Dietrich, V. J., Holloway, J. R., and Boudreau, A. E., 1989, Carbon distribution in the Stillwater Complex and evolution of vapor during crystallization of Stillwater and Bushveld magmas: Journal of Petrology, v. 30, p. 153–173.
Mathez, E. A., Duba, A. G., Peach, C. L., Leger, A., Shankland, T. J., and Plafker, G., 1995, Electrical conductivity and carbon in metamorphic rocks of the Yukon-Tanana Terrane, Alaska: Journal of Geophysical Research B, Solid Earth and Planets, v. 100, p. 10, 187–10,196.
Mattey, D. P., Carr, R. H., Wright, I. P., and Pillinger, C. T., 1984, Carbon isotopes in submarine basalts: Earth and Planetary Science Letters, v. 70, p. 196–206.
Morgan, G. B., Chou, I. M., and Pasteris, J. D., 1992, Speciation in experimental C-O-H fluids produced by the thermal dissociation of oxalic acid dihydrate: Geochimica et Cosmochimica Acta, v. 56, p. 281–294.
Morgan, G. B., Chou, I. M., Pasteris, J. D., and Olsen, S. N., 1993, Re-equilibration of $CO_2$ fluid inclusions at controlled hydrogen fugacities: Journal of Metamorphic Geology, v. 11, p. 155–164.
Newton, R. C., Smith, J. V., and Windley, B. F., 1980, Carbonic metamorphism, granulites and crustal growth: Nature, v. 288, p. 45–50.
Oberlin, A., Boulmier, J. L., and Villey, M., 1980, Electron microscope study of kerogen microtexture. Selected criteria for determining the evolution path and evolution stage of kerogen, in Durand, B., editor, Kerogen: Paris, Editions Technip, p. 191–240.
Oh, J. H., Rouzaud, J. N., Oberlin, A., Deurbergue, A., and Kwak, Y. H., 1991, Structural study of graphitization in the Moongyeong coalfield, South Korea: Bulletin Société Géologique dé France, v. 162, p. 399–407.
Ohmoto, H., and Kerrick, D. M., 1977, Devolatilization equilibria in graphitic systems: American Journal of Science, v. 277, p. 1013–1044.
Pasteris, J. D., 1981, Occurrence of graphite in serpentinized olivines in kimberlites: Geology, v. 9, p. 356–359.
—— 1984, Secondary graphitization in crustal xenolithic rocks: Geology, v. 16, p. 804–807.
—— 1989, Methane-nitrogen fluid inclusions in igneous rocks from the Duluth Complex, Minnesota: Pan-American Conference on Fluid Inclusions Research, 2nd, Program and Abstracts, p. 51.
Pasteris, J. D., and Chou, I. M., 1998, Fluid-deposited graphitic inclusions in quartz: Comparison between KTB (German continental deep-drilling) core samples and artificially re-equilibrated natural inclusions: Geochimica et Cosmochimica Acta, v. 62, p. 109–122.
Pasteris, J. D., Harris, T. N., and Sassani, D. C., 1995, Interactions of mixed volatile-brine fluids in rocks of the southwestern footwall of the Duluth Complex, Minnesota: Evidence from aqueous fluid inclusions: American Journal of Science, v. 295, p. 125–172.
Pasteris, J. D., and Luque, F. J., 1997, Why is the graphite in large epigenetic deposits of uniformly high crystallinity?: Geological Society of America Abstracts with Programs, v. 28, p. A-91.
Pasteris, J. D., and Wanamaker, B. J., 1988, Laser Raman microprobe analysis of experimentally re-equilibrated fluid inclusions in olivine: Some implications for mantle fluids: American Mineralogist, v. 73, p. 1074–1088.
Pasteris, J. D., and Wopenka, B., 1991, Raman spectra of graphite as indicators of degree of metamorphism: Canadian Mineralogist, v. 29, p. 1–9.
Pearson, D. G., Boyd, F. R., Haggerty, S. E., Pasteris, J. D., Field, S. W., Nixon, P. H., and Pokhilenko, N. P., 1994, The characterisation and origin of graphite in cratonic lithospheric mantle: a petrological carbon isotope and Raman spectroscopic study: Contributions to Mineralogy and Petrology, v. 115, p. 449–466.
Pearson, D. G., Boyd, F. R., and Nixon, P. H., 1990, Graphite-bearing mantle xenoliths from the Kaapvaal craton: implications for graphite and diamond genesis: Carnegie Institute Washington Yearbook, p. 11–19.
Pearson, D. G., Davies, G. R., Nixon, P. H., and Milledge, H. J., 1989, Graphitized diamonds from a peridotite massif in Morocco and implications for anomalous diamond occurrences: Nature, v. 338, p. 60–62.
Pineau, F., Javoy, M., and Kornprobst, J., 1987, Primary igneous graphite in ultramafic xenoliths: II. Isotopic composition of the carbonaceous phases present in xenoliths and host lava at Tissemt (Algerian Sahara): Journal of Petrology, v. 28, p. 313–322.
Reed, M. H., and Spycher, N. F., 1985, Boiling, cooling, and oxidation in epithermal systems: A numerical modeling approach, *in* Berger, B. R., and Bethke, P. M., editors, Geology and Geochemistry of Epithermal Systems: Reviews in Economic Geology, v. 2, p. 249–272.

Reutel, C., Skrotzki, W., Vollbrecht, A., 1989, TEM and RMP studies of graphites of the pilot borehole and associated field, *in* Emmermann, R., and Giese, P., editors, Kontinentales Tiefbohrprogramm der Bundesrepublik Deutschland, Report 89-3: Hannover, Germany, Niedersächsisches Landesamt für Bodenforschung, p. 445.

Ross, J. V., and Bustin, R. M., 1990, The role of strain energy in creep graphitization of anthracite: Nature, v. 343, p. 58–60.

Rumble, D., Duke, E. F., and Hoering, T. C., 1986, Hydrothermal graphite in New Hampshire: Evidence of carbon mobility during regional metamorphism: Geology, v. 14, p. 452–455.

Rumble, D., and Hoering, T. C., 1986, Carbon isotope geochemistry of graphite vein deposits from New Hampshire, U.S.A.: Geochimica et Cosmochimica Acta, v. 50, p. 1239–1247.

Santosh, M., and Wada, H., 1993, A carbon isotope study of graphites from the Kerala khondalite belt, Southern India: Evidence for $CO_2$ infiltration in granulites: Journal of Geology, v. 101, p. 643–651.

Scheele, N., and Hoefs, J., 1992, Carbon isotope fractionation between calcite, graphite and $CO_2$: an experimental study: Contributions to Mineralogy and Petrology, v. 112, p. 35–45.

Schulze, D. J., Valley, J. W., Viljoen, K. S., Stiefenhofer, J., and Spiegel, M., 1997, Carbon isotope composition of graphite in mantle eclogites: Journal of Geology, v. 105, p. 379–386.

Shengelia, D. M., Ashvetiani, R. A., and Kekskhueli, D. N., 1979, The graphite geothermometer: Academii Nauk SSSR Doklady, v. 235, p. 132–134.

Skrotzki, W., and Reutel, C., 1989, Contribution of crystallinity studies to unravel graphite formation in the Oberpfalz, *in* Emmermann, R., and Giese, P., editors, Kontinentales Tiefbohrprogramm der Bundesrepublik Deutschland, Report 90-4: Hannover, Germany, Niedersächsisches Landesamt für Bodenforschung, p. 324–332.

Soman, K., Lobzova, R. V., and Sivadas, K. M., 1986, Geology, genetic types and origin of graphite in South Kerala, India: Economic Geology, v. 81, p. 997–1002.

Stevens, G., 1997, Melting, carbonic fluids and water recycling in the deep crust: an example from the Limpopo Belt, South Africa: Journal of Metamorphic Geology, v. 15, p. 141–154.

Strens, R. G. J., 1965, The graphite deposit of Seathwaite in Borrowdale, Cumberland. Geological Magazine, v. 102, p. 393–406.

Sugisaki, R., and Mimura, K., 1994, Mantle hydrocarbons: Abiotic or biotic? Geochimica et Cosmochimica Acta, v. 58, p. 2527–2542.

Taylor, B. E., 1986, Magmatic volatiles: Isotopic variation of C, H, and S, *in* Valley, J. W., Taylor, H. P., and O'Neil, J. R., editors, Stable Isotopes in High Temperature Geological Processes: Reviews in Mineralogy, v. 16, p. 185–225.

Tingle, T. N., Mathez, E. A., and Hochella, M. F., 1991, Carbonaceous matter in peridotites and basalts studied by XPS, SALI, and LEED: Geochimica et Cosmochimica Acta, v. 55, p. 1145–1152.

Tuinstra, F., and Koenig, J. L., 1970, Raman spectrum of graphite: Journal of Chemical Physics, v. 53, p. 1126–1130.

Valley, J. W., and O'Neil, J. R., 1981, $^{13}C/^{12}C$ exchange between calcite and graphite: a possible thermometer in Grenville marbles: Geochimica et Cosmochimica Acta, v. 45, p. 411–419.

Volborth, A., and Housley, R. M., 1984, A preliminary description of complex graphite, sulphide, arsenide, and platinum group element mineralization in a pegmatoid pyroxenite of the Stillwater Complex, Montana, U.S.A.: Tschermaks Mineralogische and Petrographische Mitteilungen, v. 33, p. 213–230.

Wada, H., and Suzuki, K., 1983, Carbon isotopic thermometers calibrated by dolomite-calcite solvus temperatures: Geochimica et Cosmochimica Acta, v. 47, p. 697–706.

Wada, H., Tomita, T., Matsuura, K., Iuchi, K., Ito, M., and Morikiyo, T., 1994, Graphitization of carbonaceous matter during metamorphism with references to carbonate and pelitic rocks of contact and regional metamorphisms, Japan: Contributions to Mineralogy and Petrology, v. 118, p. 217–228.

Walther, J., and Althaus, E., 1993, Graphite deposition in tectonically mobilized fault planes of the KTB-pilot drill hole, *in* Emmermann, R., Lauterjung, J., and Umsonst, T., editors, Kontinentales Tiefbohrprogramm der Bundesrepublik Deutschland, Report 93-2: Hannover, Germany, Niedersächsisches Landesamt für Bodenforschung, p. 493–497.

Wang, G. F., 1989, Carbonaceous material in the Ryoke metamorphic rocks, Kinki district, Japan: Lithos, v. 22, p. 305–316.

Weis, P. L., Friedman, I., and Gleason, J. P., 1981, The origin of epigenetic graphite: evidence from isotopes: Geochimica et Cosmochimica Acta, v. 45, p. 2325–2332.

Wintsch, R. P., O'Connell, A. F., Ransom, B. L., and Wiechmann, M. J., 1981, Evidence for the influence of $fCH_4$ on the crystallinity of disseminated carbon in greenschist facies rocks, Rhode Island, USA: Contributions to Mineralogy and Petrology, v. 77, p. 207–213.

Wopenka, B., and Pasteris, J. D., 1993, Structural characterization of kerogens to granulite-facies graphite: Applicability of Raman microprobe spectroscopy: American Mineralogist, v. 78, p. 533–557.

Yardley, B. W. D., and Valley, J. W., 1997, The petrologic case for a dry lower crust: Journal of Geophysical Research, v. 102 (B6), p. 12173–12185.

Ziegenbein, D., and Johannes, W., 1980, Graphite in C-H-O fluids: An unsuitable compound to buffer fluid composition at temperatures up to 700°C: Neues Jahrbuch Mineralogie Monatshefte, v. 7, p. 289–305.

——— 1989, Graphite, fluid and reactions: Einfluss der Graphit ristallinität, *in* Emmermann, R., and Giese, P., editors, Kontinentales Tiefbohrprogramm der Bundesrepublik Deutschland, Report 90-4: Hannover, Germany, Niedersächsisches Landesamt für Bodenforschung, p. 559.

Ziegenbein, D., Skrotzki, R., Hoefs, J., Müller, H., Reutel, C., and Emmermann, R., 1989, Fluidzusammensetzung und Graphitbildung auf Störungszonen, *in* Emmermann, R., and Giese, P., editors, Kontinentales Tiefbohrprogramm der Bundesrepublik Deutschland, Report 89-3: Hannover, Germany, Niedersächsisches Landesamt für Bodenforschung, p. 46–53.